Distribution Category:
Nuclear Converter Reactor Fuel Cycle
Technology: Base Technology (UC-83)

ANL/RERTR/TM-5

ANL/RERTR/TM--5

DE85 002646

ARGONNE NATIONAL LABORATORY
9700 South Cass Avenue
Argonne, Illinois 60439

BLACKNESS COEFFICIENTS, EFFECTIVE DIFFUSION PARAMETERS, AND CONTROL ROD WORTHS FOR THERMAL REACTORS

by

M. M. Bretscher

RERTR Program
Applied Physics Division

September 1984

Table of Contents

List of Figures

List of Tables

Blackness Coefficients, Effective Diffusion Parameters, and Control Rod Worths for Thermal Reactors

M. M. Bretscher

RERTR Program, Applied Physics Division
Argonne National Laboratory
Argonne, Illinois 60439

ABSTRACT

Simple diffusion theory cannot be used to evaluate control rod worths in thermal reactors because of the strongly absorbing character of the control material. However, good results can be obtained from a diffusion calculation by representing the absorber slab by means of a suitable pair of internal boundary conditions. These internal boundary conditions, or "blackness coefficients," are defined by the equations

$$\alpha = \frac{J_\ell + J_r}{\phi_\ell + \phi_r} , \qquad \beta = \frac{J_\ell - J_r}{\phi_\ell - \phi_r}$$

where ϕ and J are the asymptotic values of the neutron flux and current <u>into</u> the slab on the left-hand and right-hand surfaces. Mesh-dependent effective diffusion parameters (D, Σ_a) for the control slab are obtained from the blackness coefficients.

Methods for calculating α and β in the P_1, P_3, and P_5 approximations, with and without scattering, are presented. By appropriately weighting the fine-group blackness coefficients, broad group values, $\langle\alpha\rangle$ and $\langle\beta\rangle$, are obtained.

The technique is applied to the calculation of control rod worths of Cd, Ag-In-Cd, and Hf control elements. Results are found to compare very favorably with detailed Monte Carlo calculations.

For control elements whose geometry does not permit a thin slab treatment, other methods are needed for determining the effective diffusion parameters. One such method is briefly discussed and applied to the calculation of control rod worths in the Ford Nuclear Reactor at the University of Michigan. Calculated and measured worths are found to be in good agreement.

List of Tables (Continued)

Blackness Coefficients, Effective Diffusion Parameters, and Control Rod Worths for Thermal Reactors

1. INTRODUCTION

In strongly absorbing media the neutron flux is a rapidly varying function of position. Under these circumstances Fick's law of diffusion is invalid and so diffusion theory cannot be used to evaluate control rod worths in thermal neutron reactors. However, blackness theory provides a method for modifying diffusion parameters in strongly absorbing media so that diffusion theory may be used in regions where it would normally be inadequate. Two blackness coefficients, α and β, are defined by the equations

$$\alpha = \frac{J_\ell + J_r}{\phi_\ell + \phi_r} , \qquad \beta = \frac{J_\ell - J_r}{\phi_\ell - \phi_r}$$

where ϕ_ℓ and ϕ_r are the asymptotic neutron fluxes on the left-hand and right-hand surfaces of the absorber slab and the J's are the net surface currents <u>into</u> the slab. These blackness coefficients form a pair of internal boundary conditions at the surfaces of the absorber slab and may be evaluated from one-dimensional transport calculations. Effective diffusion parameters, Σ_a and D, for the strongly absorbing control rod regions are determined as functions of these blackness coefficients. This blackness-modified diffusion theory permits a rather accurate calculation of control rod worths in thermal reactors for control elements whose geometry can be represented by one or more slabs.

This paper deals with the methods used to calculate the blackness coefficients in the P_1, P_3, and P_5 approximations taking into account the effects of both neutron absorption and neutron scattering within the control material. A fine-group weighting scheme is used to determine the average values of the blackness coefficients corresponding to each of the broad groups. Equations for the effective diffusion parameters are derived as functions of the broad-group blackness coefficients. Finally, the method is used to evaluate control rod worths for several different geometries and compositions, and the results are compared with those obtained from detailed continuous energy Monte Carlo calculations.

For control elements which cannot be described in terms of slab geometry, quantities analogous to α and β do not exist. For this case, however, a different method may be used to find effective diffusion parameters for such lumped absorbers. This technique is described at the end of this report and is used to evaluate control rod worths in the Ford Nuclear Reactor at the University of Michigan. Results are compared with measured values.

2. THE ASSUMPTIONS OF BLACKNESS THEORY

From the outset it is well to list the assumptions upon which blackness theory rests.

1. The control slab is assumed to be uniform and of infinite lateral extent.

and

$$T_{mn}(\Sigma_t\tau, \Sigma_s/\Sigma_t) = \int_0^1 \mu^m \psi_n(\tau,\mu)d\mu. \qquad (2)$$

R_{mn} and T_{mn} are the reflected and transmitted contributions to the outgoing m^{th} moments due to the incoming flux.

With a μ^n source distribution, the ONEDANT Code[2] is used to solve the monoenergetic one-dimensional Boltzmann equation for the surface fluxes $\psi_n(0,\mu)$ and $\psi_n(\tau,\mu)$. These calculations are done using an angular quadrature order of 24 (i.e. S_{24}) and double P_N quadrature constants.

With the ONEDANT values for the surface fluxes $\psi_n(0,\mu)$ and $\psi_n(\tau,\mu)$, Eqs. (1) and (2) are numerically integrated by Gauss-Legendre quadrature methods[3] to obtain R_{mn} and T_{mn}. By using the double P_N quadrature constants in the ONEDANT calculations, the angular fluxes are evaluated at the required Gaussian abscissas μ_i so that the Gauss-Legendre quadrature method gives

$$R_{mn} = (-1)^m \sum_{i=1}^{N/2} \mu_i^m \psi_n(0,\mu_i)W_i, \qquad \mu<0$$

$$T_{mn} = \sum_{i=1}^{N/2} \mu_i^m \psi_n(\tau,\mu_i)W_i, \qquad \mu>0$$

where W_i are the required Gauss-Legendre weights (see Table I) and N is the angular quadrature order (S_N).

In general, the reflection and transmission coefficients must be obtained numerically. However, for the special case of a pure absorber ($\Sigma_s = 0$) R_{mn} is zero and T_{mn} can be expressed analytically. For this case the transmitted angular flux is the product of the incident flux and the probability of passing through the slab without absorption. Thus,

$$\psi_n(\tau,\mu) = \mu^n e^{-\Sigma_a\tau/\mu}, \qquad \mu>0$$

$$= 0, \qquad \mu<0 .$$

Thus,

$$T_{mn}(\Sigma_a\tau) = \int_0^1 \mu^{m+n} e^{-\Sigma_a\tau/\mu} d\mu$$

$$= E_{m+n+2}(\Sigma_a\tau)$$

where $E_{m+n+2}(\Sigma_a\tau)$ is the exponential integral of order m+n+2.

A computer program has been written to evaluate the reflection and transmission coefficients using the angular flux output file from ONEDANT. To check these numerical methods, R_{mn} and T_{mn} were calculated for $\Sigma_t\tau$ and Σ_s/Σ_t values corresponding to tabulated values of R_{mn} and T_{mn} given by Maynard.[4] Results are compared in Table II. It is seen that the agreement is quite satisfactory. For the pure absorption case, the numerical results agree with the tabulated values of the exponential integral[5] to within 0.001%.

Table I. Gauss-Legendre Abscissas and Weights

($S_N = S_{24}$)

Absciassas, μ_i	Weights, W_i
±0.99078	0.023588
±0.95206	0.053470
±0.88495	0.080039
±0.79366	0.10158
±0.68392	0.11675
±0.56262	0.12457
±0.43738	0.12457
±0.31608	0.11675
±0.20634	0.10158
±0.11505	0.080039
±0.047941	0.053470
±0.0092197	0.023588

Table II. Comparison with Maynard Values[4] for R_{mn} and T_{mn}.

$\Sigma_t\tau = 2.50, \qquad \Sigma_s/\Sigma_t = 0.40$

Source	n	R_{1n}	R_{3n}	T_{1n}	T_{3n}
Maynard	0	0.053552	0.023810	0.026897	0.017915
ONEDANT, etc.	0	0.053539	0.023811	0.026901	0.017930
Maynard	1	0.033099	0.014947	0.021450	0.014765
ONEDANT, etc.	1	0.033100	0.014946	0.021462	0.014775
Maynard	2	0.023810	0.010830	0.017915	0.012676
ONEDANT, etc.	2	0.023810	0.010829	0.017930	0.012681
Maynard	3	0.018553	0.0084735	0.015403	0.011145
ONEDANT, etc.	3	0.018554	0.0084733	0.015415	0.011148

$\Sigma\tau = 1.50, \qquad \Sigma_s/\Sigma = 0.0$

Maynard	0	0.0	0.0	0.056751	0.038527
ONEDANT, etc.	0	0.0	0.0	0.056739	0.038530
$E_{m+n+2}(1.50)$*	0			0.056739	0.038530

*From tables of the exponential integral given in Ref. 5.

4. MATCHING BOUNDARY CONDITIONS

Before obtaining expressions for the blackness coefficients α and β, it is necessary to consider matching conditions imposed at the surfaces of the absorber slab. Consider the three-region slab configuration shown below in which the central region extends over the interval $0 < x < \tau$.

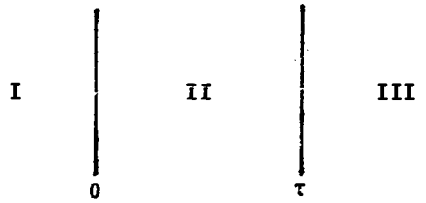

Three-Region Slab Configuration

The angular fluxes incident on Region II from Regions I and III must be continuous at the boundaries.

$$\psi_{II}(0,\mu) = \psi_I(0,\mu), \qquad \mu>0$$

$$\psi_{II}(\tau,\mu) = \psi_{III}(\tau,\mu), \qquad \mu<0$$

The moments of the distributions leaving Region II ($\psi_{II}(0,\mu)$, $\mu<0$ and $\psi_{II}(\tau,\mu)$, $\mu>0$) are determined from the incident distributions by means of the reflection and transmission coefficients.

Suppose the boundary fluxes in Regions I and III are expanded into a power series over the full range of μ(-1 to 1).

$$\psi_I(0,\mu) = \sum_{n=0}^{L} A_n \mu^n \tag{3}$$

$$\psi_{III}(\tau,\mu) = \sum_{n=0}^{L} B_n \mu^n \tag{4}$$

This expansion is equivalent to the P_L approximation.

If Region II is a source-free medium which scatters neutrons isotropically, Maynard[1] has shown that the matching conditions become

$$\sum_{n=0}^{L} \left[\left(\frac{(-1)^n}{m+n+1} - R_{mn}\right) A_n - (-1)^n T_{mn} B_n\right] = 0 \tag{5}$$

and

$$\sum_{n=0}^{L} \left[\left(\frac{1}{m+n+1} - (-1)^n R_{mn}\right) B_n - T_{mn} A_n\right] = 0 \tag{6}$$

It turns out that either the even or the odd moments can be matched. The odd moments are usually chosen. Thus, only odd values of m need be considered in Eqs. (5) and (6) with $m_{max} = L$.

An important special case is obtained by taking the center line of Region II as an axis of symmetry. For this case

$$A_n = (-1)^n B_n$$

and Eqs. (3) and (4) reduce to

$$\sum_{n=0}^{L} \left[\frac{1}{m + n + 1} - (-1)^n (R_{mn} + T_{mn}) \right] B_n = 0 \tag{7}$$

at either boundary. As discussed earlier, for the no scattering case $R_{mn} = 0$ and $T_{mn} = E_{m+n+2}$ and one can show that Eq. (7) leads to the boundary conditions considered by Royston.[6]

5. EVALUATION OF THE BLACKNESS COEFFICIENTS

The blackness coefficients α and β were first introduced by Goldsmith, et al.[7] and are defined by the equations

$$\alpha \equiv \frac{J_\ell + J_r}{\phi_\ell + \phi_r} \tag{8}$$

$$\beta \equiv \frac{J_\ell - J_r}{\phi_\ell - \phi_r} \tag{9}$$

where J_ℓ and J_r are the net asymptotic neutron currents <u>into</u> the slab from the left and right sides respectively and ϕ_ℓ and ϕ_r the asymptotic fluxes at the left and right boundaries of the slab. Note that β is indeterminate if the center of the plate is a plane of symmetry. For this case α is the surface current-to-flux ratio and corresponds to the internal boundary condition in the DIF3D code.[8]

To obtain expressions for α and β the angular fluxes to the left and right of the absorber plate are expanded in a Legendre series, which in the P_L approximation becomes

$$\psi(x,\mu) \approx \frac{1}{2} \sum_{n=0}^{L} (2n+1)\ \psi_n(x)\ P_n(\mu). \tag{10}$$

Before continuing with the evaluation of the blackness coefficients, we must first determine the spherical harmonic moments, $\psi_n(x)$, corresponding to the one-dimensional monoenergetic Boltzmann transport equation.

5.1 Evaluation of the Spherical Harmonic Moments of the Angular Flux Distribution

In the medium outside the control blade the monoenergetic, one-dimensional, time-independent transport equation for plane geometry, in the absence of sources, is

$$\mu \frac{\partial}{\partial x} \psi(x,\mu) + \Sigma_t \psi(x,\mu) = \frac{1}{2} \int_{-1}^{1} [\Sigma_s(\mu_0) + \frac{\bar{\nu}\Sigma_f}{k_{eff}}] \psi(x,\mu')d\mu' \qquad (11)$$

where

x	is the position coordinate,
μ	is the cosine of the angle between the direction of the neutron velocity and the x axis,
$\psi(x,\mu)d\mu$	is the flux between μ and $\mu + d\mu$,
μ_0	is the cosine of the angle between the incident and scattered neutron velocities,
$\Sigma_t, \Sigma_s, \Sigma_f$	the macroscopic total, scattering, and fission cross sections, respectively,
$\bar{\nu}$	is the average number of neutrons per fission,
k_{eff}	is the effective multiplication factor. This is needed to make the Boltzmann equation time-independent.

Now the flux and the differential scattering cross section are expanded in spherical harmonics.

$$\psi(x,\mu) = \frac{1}{2} \sum_{n=0}^{\infty} (2n + 1)\psi_n(x)P_n(\mu)$$

$$\Sigma_s(\mu_0) = \frac{1}{2} \sum_{n=0}^{\infty} (2n + 1)\Sigma_{sn}P_n(\mu_0)$$

where $P_n(\mu)$ is the nth order Lengendre polynomial. In these last equations

$$\psi_n(x) = \int_{-1}^{1} \psi(x,\mu)P_n(\mu)d\mu$$

$$\Sigma_{sn} = \int_{-1}^{1} \Sigma_s(\mu_0)P_n(\mu_0)d\mu_0$$

The quantities $\psi_n(x)$ are called the spherical harmonic moments of the angular flux distribution $\psi(x,\mu)$. The first two moments, $\psi_0(x)$ and $\psi_1(x)$, are identical to the flux $\phi(x)$ and the current $j(x)$, respectively.

Using the above expansions, Eq. (11) is multiplied by $(2n + 1)P_n(\mu)$ and integrated over all μ. This results in a coupled set of linear differential equations for the spherical harmonic moments $\psi_n(x)$. Using the recurrence formula

$$(n + 1)P_{n+1}(\mu) + nP_{n-1}(\mu) = (2n + 1)\mu P_n(\mu),$$

it follows that

$$\lambda(n+1)\psi'_{n+1}(x) + \lambda n\psi'_{n-1}(x) + (2n + 1)\left[b_n - \frac{\overline{\nu}\Sigma_f}{k_{eff}\Sigma_t}\delta_{0n}\right]\psi_n(x) = 0 \qquad (12)$$

$$n = 0, 1, 2, \ldots, \infty$$

where $\lambda = 1/\Sigma_t$ is the total mean free path in the medium and where

$$b_n = \frac{\Sigma_t - \Sigma_{sn}}{\Sigma_t}, \quad b_0 = \frac{\Sigma_t - \Sigma_s}{\Sigma_t} = \Sigma_a/\Sigma_t .$$

If the scattering is isotropic, $\Sigma_{sn} = 0$ for $n > 0$ and so $b_n = 1$ for $n > 0$. The primes in Eq. (12) denote differentiation with respect to x. In general, the scattering cross section may be written in terms of a frequency function $f(\mu_0)$.

$$\Sigma_s(\mu_0) = \Sigma_s f(\mu_0),$$

where $f(\mu_0)d\mu_0$ is the fraction of all scattering collisions which result in scattering angles whose cosines lie between μ_0 and $\mu_0 + d\mu_0$. In the linear anisotropic scattering approximation,

$$f(\mu_0) = \frac{1}{2}(1 + 3\,\overline{\mu}_0\mu_0)$$

and so

$$\Sigma_{sn} = \int_{-1}^{1} \Sigma_s(\mu_0)P_n(\mu_0)d\mu_0 = \Sigma_s \int_{-1}^{1} \frac{1}{2}(1 + 3\,\overline{\mu}_0\mu_0)P_n(\mu_0)d\mu_0$$

$$= \Sigma_s \text{ for } n = 0$$

$$= \overline{\mu}_0\Sigma_s \text{ for } n = 1$$

$$= 0 \text{ for } n > 1 .$$

For this case,

$$b_0 = \frac{\Sigma_t - \Sigma_{s_0}}{\Sigma_t} = \Sigma_a/\Sigma_t$$

$$b_1 = \frac{\Sigma_t - \overline{\mu}_0\Sigma_s}{\Sigma_t} = \frac{\Sigma_a + \Sigma_s(1 - \overline{\mu}_0)}{\Sigma_t} = \Sigma_{tr}/\Sigma_t$$

$$b_n = 1 \text{ for } n > 1$$

where Σ_{tr} is the macroscopic transport cross section.

Equation (12) represents an infinite set of coupled differential equations. Though rigorous, they are not very useful unless approximations are made. In the P_L approximation, the series expansion for $\psi(\mu,x)$ is truncated with the L_{th} term:

$$\psi(x,\mu) \approx \frac{1}{2}\sum_{n=0}^{L}(2n+1)\psi_n(x)P_n(\mu)$$

where $\psi_n(x) = 0$ for $n > L$. Thus, in the P_L approximation Eq. (12) becomes

$$\begin{aligned} &\lambda\psi_1'(x) + \bar{\alpha}\psi_0(x) = 0 \\ &\lambda(n+1)\psi_{n+1}'(x) + \lambda n\psi_{n-1}' + (2n+1)b_n\psi_n(x) = 0, \quad n = 1, 2, \ldots, L-1 \\ &\lambda L\psi_{L-1}'(x) + (2L+1)b_L\,\psi_L(x) = 0 \end{aligned} \tag{13}$$

where

$$\bar{\alpha} \equiv b_0 - \frac{\bar{\nu}\Sigma_f}{k_{eff}\Sigma_t} = \frac{\Sigma_t - (\Sigma_s + \bar{\nu}\Sigma_f/k_{eff})}{\Sigma_t} = \frac{\Sigma_a - \bar{\nu}\Sigma_f/k_{eff}}{\Sigma_t}.$$

For reasons not discussed here (see Ref. 9), odd values of L lead to more accurate results than those obtained with the next P_{L+1} approximation.

We seek solutions to Eq. (13) of the form

$$\psi_n(x) = g_n(\nu)e^{\nu x/\lambda}. \tag{14}$$

Substituting this into Eq. (13) leads to the recurrence relation for the $g_n(\nu)$'s.

$$\nu[(n+1)g_{n+1}+ng_{n-1}] + [(2n+1)b_n - \frac{\bar{\nu}\Sigma_f}{k_{eff}\Sigma_t}\delta_{0n}]g_n = 0 \tag{15}$$

where, by definition, $g_0(\nu) = 1$. Equation (15) shows that $g_1(\nu) = -\bar{\alpha}/\nu$. It follows from Eq. (15) that $g_n(-\nu) = (-1)^n g_n(\nu)$. In the P_L approximation, $\psi_{L+1}(x) = 0$ which requires that $g_{L+1}(\nu) = 0$. This last equation determines the allowed values of ν in Eq. (14). Equation (15) is compatible only if the determinant of the coefficients vanishes. This condition provides an alternate method for finding the roots ν_i. Thus, the ν_i's are the positive roots of the determinental equation

$$
\begin{vmatrix}
\bar{\alpha} & \nu & 0 & 0 & 0 & 0 & \cdots & 0 & 0 \\
\nu & 3b_1 & 2\nu & 0 & 0 & 0 & \cdots & 0 & 0 \\
0 & 2\nu & 5b_2 & 3\nu & 0 & 0 & \cdots & 0 & 0 \\
0 & 0 & 3\nu & 7b_3 & 4\nu & 0 & \cdots & 0 & 0 \\
0 & 0 & 0 & 4\nu & 9b_4 & 5\nu & \cdots & 0 & 0 \\
0 & 0 & 0 & 0 & 5\nu & 11b_5 & \cdots & 0 & 0 \\
\cdots & \cdots & \cdots & \cdots & \cdots & \cdots & \cdots & \cdots & \cdots \\
0 & 0 & 0 & 0 & 0 & 0 & \cdots & (L-1)\nu & 0 \\
0 & 0 & 0 & 0 & 0 & 0 & \cdots & (2L-1)b_{L-1} & L\nu \\
0 & 0 & 0 & 0 & 0 & 0 & \cdots & L\nu & (2L+1)b_L
\end{vmatrix} = 0 \quad (16)
$$

such that $0 < \nu_i < \nu_{i+1}$. Recall that $\bar{\alpha} = (\Sigma_a - \bar{\nu}\Sigma_f/k_{eff})/\Sigma_t$ and that for linear anisotropic scattering $b_0 = \Sigma_a/\Sigma_t$, $b_1 = \Sigma_{tr}/\Sigma_t$ and $b_n = 1$ for $n > 1$. For calculating higher order effects it is a good approximation to assume that the control blade is surrounded by a homogenized fuel region of infinite extent. Then, consistent with the one-group infinite medium model,

$$k_{eff} = k_\infty = \bar{\nu}\Sigma_f/\Sigma_a$$

and $\bar{\alpha} = (\Sigma_a - \bar{\nu}\Sigma_f/k_{eff})/\Sigma_t = (\Sigma_a - \Sigma_a)/\Sigma_t = 0$.

If we take the $x = 0$ reference plane at the center of the absorber plate, the general solution for the spherical harmonic moments is obtained from Eq. (14) by summing over the permissible values of ν. The result can be written in the form

$$\psi_n(x) = \phi\,\delta_{0n} + j\,\delta_{1n} + \sum_{i=2}^{\frac{1}{2}(L+1)} g_n(\nu_i)\, a_i' e^{\nu_i x/\lambda}, \quad x<0 \qquad (17a)$$

and

$$\psi_n(x) = \phi\,\delta_{0n} + j\,\delta_{1n} + (-1)^n \sum_{i=2}^{\frac{1}{2}(L+1)} g_n(\nu_i)\, b_i' e^{-\nu_i x/\lambda}, \quad x>0 \qquad (17b)$$

where $n=0, 1, \ldots, L$, and where a_i' and b_i' are arbitrary constants to be determined from boundary conditions.

With these relations the blackness coefficients can be evaluated in the P_L approximation for successive values of L.

5.2 Blackness Coefficients in the P_1 Approximation

In the P_1 approximation Eqs. (3), (4), (10) and (17) reduce to

$$\psi_\ell \equiv \psi_I(0,\mu) = A_0 + A_1\,\mu = \frac{1}{2}\,\psi_0 + \frac{3}{2}\,\psi_1\,\mu = \frac{1}{2}\,\phi_\ell + \frac{3}{2}\,j_\ell\,\mu$$

$$\psi_r \equiv \psi_{III}(\tau,\mu) = B_0 + B_1\mu = \frac{1}{2}\,\phi_r + \frac{3}{2}\,j_r\,\mu .$$

Hence,

$$A_0 = \frac{1}{2}\,\phi_\ell\ , \qquad A_1 = \frac{3}{2}\,j_\ell$$

$$B_0 = \frac{1}{2}\,\phi_r\ , \qquad B_1 = \frac{3}{2}\,j_r .$$

Note the j_ℓ and j_r are the neutron currents at the surfaces of the absorber slab and, therefore, $j_\ell = J_\ell$ and $j_r = -J_r$.

For L = 1, the matching conditions (Eqs. 5 and 6) become

$$(\tfrac{1}{2} - R_{10})A_0 - T_{10}\,B_0 - (\tfrac{1}{3} + R_{11})A_1 + T_{11}\,B_1 = 0$$

$$(\tfrac{1}{2} - R_{10})B_0 - T_{10}\,A_0 + (\tfrac{1}{3} + R_{11})B_1 - T_{11}\,A_1 = 0$$

Adding these equations, rearranging terms, and using the expressions for the A's and B's one obtains

$$\frac{A_1 - B_1}{A_0 + B_0} = \frac{\frac{1}{2} - R_{10} - T_{10}}{\frac{1}{3} + R_{11} + T_{11}} = \frac{\frac{3}{2}\,(j_\ell - j_r)}{\frac{1}{2}\,(\phi_\ell + \phi_r)} .$$

Hence,

$$\alpha \equiv \frac{J_\ell + J_r}{\phi_\ell + \phi_r} = \frac{j_\ell - j_r}{\phi_\ell + \phi_r} = \frac{\frac{1}{2}\,[1 - 2\,R_{10} - 2\,T_{10}]}{[1 + 3\,R_{11} + 3\,T_{11}]} . \tag{18}$$

By subtracting the two equations for the matching conditions it follows that

$$\frac{A_1 + B_1}{A_0 - B_0} = \frac{\frac{1}{2} - R_{10} + T_{10}}{\frac{1}{3} + R_{11} - T_{11}} = \frac{\frac{3}{2}\,(j_\ell + j_r)}{\frac{1}{2}\,(\phi_\ell - \phi_r)} .$$

and so

$$\beta \equiv \frac{J_\ell - J_r}{\phi_\ell - \phi_r} = \frac{j_\ell + j_r}{\phi_\ell - \phi_r} = \frac{\frac{1}{2}\,[1 - 2\,R_{10} + 2\,T_{10}]}{[1 + 3\,R_{11} - 3\,T_{11}]}\,. \tag{19}$$

Note that in the P_1 approximation α and β depend only on the properties ($\Sigma_t\tau$ and Σ_s/Σ_t) of the absorber slab (see Eqs. 1 and 2).

5.3 Blackness Coefficients in the P_3 Approximation

The same methods are used to evaluate α and β in the P_3 approximation. From Eqs. (3) and (10) with $L = 3$ and the expressions for the Legendre polynomials,

$$\psi_\ell \equiv \psi_I(0,\mu) = \frac{1}{2}\,\psi_{0\ell}\,P_o + \frac{3}{2}\,\psi_{1\ell}P_1 + \frac{5}{2}\,\psi_{2\ell}P_2 + \frac{7}{2}\,\psi_{3\ell}P_3$$

$$= (\frac{1}{2}\,\psi_{0\ell} - \frac{5}{4}\,\psi_{2\ell}) + (\frac{3}{2}\,\psi_{1\ell} - \frac{21}{4}\,\psi_{3\ell})\mu + \frac{15}{4}\,\psi_{2\ell}\,\mu^2 + \frac{35}{4}\,\psi_{3\ell}\,\mu^3$$

$$= A_0 + A_1\,\mu + A_2\,\mu^2 + A_3\,\mu^3$$

A similiar equation applies to the right side of the slab so that

$$A_0 = \frac{1}{2}\,\psi_{0\ell} - \frac{5}{4}\,\psi_{2\ell} \qquad B_0 = \frac{1}{2}\,\psi_{0r} - \frac{5}{4}\,\psi_{2r}$$

$$A_1 = \frac{3}{2}\,\psi_{1\ell} - \frac{21}{4}\,\psi_{3\ell} \qquad B_1 = \frac{3}{2}\,\psi_{1r} - \frac{21}{4}\,\psi_{3r}$$

$$A_2 = \frac{15}{4}\,\psi_{2\ell} \qquad B_2 = \frac{15}{4}\,\psi_{2r}$$

$$A_3 = \frac{35}{4}\,\psi_{3\ell} \qquad B_3 = \frac{35}{4}\,\psi_{3r}$$

It follows from Eqs. (17a) and (17b) that

$$\psi_{0\ell} = \phi_\ell + a \qquad \psi_{0r} = \phi_r + b$$

$$\psi_{1\ell} = j_\ell + g_1(\nu_2)a \qquad \psi_{1r} = j_r - g_1(\nu_2)b$$

$$\psi_{2\ell} = g_2(\nu_2)a \qquad \psi_{3r} = g_2(\nu_2)b$$

$$\psi_{3\ell} = g_3(\nu_2)a \qquad \psi_{3r} = -\,g_3(\nu_2)b$$

where $a \equiv a_2' \, e^{-\nu_2 \tau/2\lambda}$, $b \equiv b_2' \, e^{-\nu_2 \tau/2\lambda}$, ν_2 is the largest positive root of Eq. (16) with $L = 3$, and the g's are given by the recurrence relation, Eq. 15. From these equations it follows that

$$
\begin{aligned}
A_0 \pm B_0 &= \frac{1}{2}(\phi_\ell \pm \phi_r) + \frac{1}{2}(a \pm b)[1 - \frac{5}{2} g_2(\nu_2)] \\
A_1 \mp B_1 &= \frac{3}{2}(j_\ell \mp j_r) + \frac{3}{2}(a \pm b)[g_1(\nu_2) - \frac{7}{2} g_3(\nu_2)] \\
A_2 \pm B_2 &= \frac{15}{4}(a \pm b)\, g_2(\nu_2) \\
A_3 \mp B_3 &= \frac{35}{4}(a \pm b)\, g_3(\nu_2)
\end{aligned}
\tag{20}
$$

If the matching conditions (Eqs. 5 and 6) are evaluated for $L = 3$ with $m = 1$ and added, one obtains

$$
\begin{aligned}
&(A_0 + B_0)[\tfrac{1}{2} - R_{10} - T_{10}] - (A_1 - B_1)[\tfrac{1}{3} + R_{11} + T_{11}] \\
&\quad + (A_2 + B_2)[\tfrac{1}{4} - R_{12} - T_{12}] - (A_3 - B_3)[\tfrac{1}{5} + R_{13} + T_{13}] = 0
\end{aligned}
\tag{21}
$$

Similarly for the $m = 3$ case, one obtains

$$
\begin{aligned}
&(A_0 + B_0)[\tfrac{1}{4} - R_{30} - T_{30}] - (A_1 - B_1)[\tfrac{1}{5} + R_{31} + T_{31}] \\
&\quad + (A_2 + B_2)[\tfrac{1}{6} - R_{32} - T_{32}] - (A_3 - B_3)[\tfrac{1}{7} + R_{33} + T_{33}] = 0
\end{aligned}
\tag{22}
$$

Now the P_3 approximation for the blackness coefficient α is obtained by substituting the results for $(A_0 + B_0)$, $(A_1 - B_1)$, $(A_2 + B_2)$, and $(A_3 - B_3)$ into Eqs. (21) and (22) and eliminating the constant $(a + b)$ from the two equations. In a similar way, by subtracting the equations for the matching conditions one obtains the P_3 approximation for the blackness coefficient β. The result for α may be written in the form

$$
\alpha = \frac{j_\ell - j_r}{\phi_\ell + \phi_r} = \frac{b_{10}\, d_3 - b_{30}\, d_1}{3\,(b_{11}\, d_3 - b_{31}\, d_1)}
\tag{23}
$$

where

$$
\begin{aligned}
d_1 &\equiv a_0\, b_{10} - a_1\, b_{11} + a_2\, b_{12} - a_3\, b_{13} \\
d_3 &\equiv a_0\, b_{30} - a_1\, b_{31} + a_2\, b_{32} - a_3\, b_{33}
\end{aligned}
$$

and

$$a_0 = \frac{1}{2}[1 - \frac{5}{2} g_2(\nu_2)] , \qquad a_1 = \frac{3}{2} [g_1(\nu_2) - \frac{7}{2} g_3(\nu_2)]$$

$$a_2 = \frac{15}{4} g_2(\nu_2) , \qquad a_3 = \frac{35}{4} g_3 (\nu_2)$$

$$b_{10} = \frac{1}{2} - R_{10} - T_{10} , \qquad b_{11} = \frac{1}{3} + R_{11} + T_{11}$$

$$b_{12} = \frac{1}{4} - R_{12} - T_{12} , \qquad b_{13} = \frac{1}{5} + R_{13} + T_{13}$$

$$b_{30} = \frac{1}{4} - R_{30} - T_{30} , \qquad b_{31} = \frac{1}{5} + R_{31} + T_{31}$$

$$b_{32} = \frac{1}{6} - R_{32} - T_{32} , \qquad b_{33} = \frac{1}{7} + R_{33} + T_{33}.$$

With L = 3, Eq. (16) determines ν_2, the largest positive root. The $g_n(\nu_2)$ functions are given by the recurrence relation (Eq. 15). An expression identical to Eq. (23) results for the blackness coefficient β except for a change in sign of the transmission coefficients, T_{mn}, in the above equations for the constants b_{mn}. Note that it is sufficient to assume linear anisotropic scattering for the purpose of evaluating the positive roots of Eq. (16).

For linear anisotropic scattering with $\bar{\alpha} = 0$, the determinental equation (Eq. 16) in the P_3 approximation reduces to

$$\begin{vmatrix} 0 & \nu & 0 & 0 \\ \nu & 3\Sigma_{tr}/\Sigma_t & 2\nu & 0 \\ 0 & 2\nu & 5 & 3\nu \\ 0 & 0 & 3\nu & 7 \end{vmatrix} = 0$$

and becomes

$$\nu^2 (9\nu^2 - 35) = 0.$$

The roots are therefore

$$\nu_i = 0, 0, \pm \frac{1}{3}\sqrt{35}$$

and so $\nu_2 = (\sqrt{35})/3 = 1.9720266$. Equation (15) determines the values of $g_n(\nu_2)$. Thus,

$$g_1(\nu_2) = -\bar{\alpha}/\nu_2 = 0$$
$$g_2(\nu_2) = -1/2$$
$$g_3(\nu_2) = 5/6\nu_2.$$

Equation (23) now gives the value of the blackness coefficient α in the P_3 approximation. The same equation but with the signs of the transmission coefficients reversed determines β. Note that for linear anisotropic scattering with $\bar{\alpha} = 0$, the P_3 blackness coefficients are independent of the properties of the external media.

5.4 Blackness Coefficients in the P_5 Approximation

In the P_5 approximation ($L = 5$) Eqs. (3) and (10) become

$$\psi_\ell = \psi_I(0,\mu) = \frac{1}{2}\psi_{0\ell} + \frac{3}{2}\psi_{1\ell} P_1 + \frac{5}{2}\psi_{2\ell} P_2 + \frac{7}{2}\psi_{3\ell} P_3 + \frac{9}{2}\psi_{4\ell} P_4 + \frac{11}{2}\psi_{5\ell} P_5$$

$$= \left(\frac{1}{2}\psi_{0\ell} - \frac{5}{4}\psi_{2\ell} + \frac{27}{16}\psi_{4\ell}\right) + \left(\frac{3}{2}\psi_{1\ell} - \frac{21}{4}\psi_{3\ell} + \frac{165}{16}\psi_{5\ell}\right)\mu$$

$$+ \left(\frac{15}{4}\psi_{2\ell} - \frac{135}{8}\psi_{4\ell}\right)\mu^2 + \left(\frac{35}{4}\psi_{3\ell} - \frac{385}{8}\psi_{5\ell}\right)\mu^3$$

$$+ \frac{315}{16}\psi_{4\ell}\mu^4 + \frac{693}{16}\psi_{5\ell}\mu^5 = \sum_{n=0}^{5} A_n \mu^n .$$

A similar equation applies to the right side of the absorber slab so that

$$A_0 = \frac{1}{2}\psi_{0\ell} - \frac{5}{4}\psi_{2\ell} + \frac{27}{16}\psi_{4\ell} , \qquad B_0 = \frac{1}{2}\psi_{0r} - \frac{5}{4}\psi_{2r} + \frac{27}{16}\psi_{4r}$$

$$A_1 = \frac{3}{2}\psi_{1\ell} - \frac{21}{4}\psi_{3\ell} + \frac{165}{16}\psi_{5\ell} , \qquad B_1 = \frac{3}{2}\psi_{1r} - \frac{21}{4}\psi_{3r} + \frac{165}{16}\psi_{5r}$$

$$A_2 = \frac{15}{4}\psi_{2\ell} - \frac{135}{8}\psi_{4\ell} , \qquad B_2 = \frac{15}{4}\psi_{2r} - \frac{135}{8}\psi_{4r}$$

$$A_3 = \frac{35}{4}\psi_{3\ell} - \frac{385}{8}\psi_{5\ell} , \qquad B_3 = \frac{35}{4}\psi_{3r} - \frac{385}{8}\psi_{5r}$$

$$A_4 = \frac{315}{16}\psi_{4\ell} , \qquad B_4 = \frac{315}{16}\psi_{4r}$$

$$A_5 = \frac{693}{16}\psi_{5\ell} , \qquad B_5 = \frac{693}{16}\psi_{5r}$$

Equations (17a) and (17b) now become

$$\psi_{0\ell} = \phi_\ell + a_2 + a_3 , \qquad \psi_{0r} = \phi_r + b_2 + b_3$$

$$\psi_{1\ell} = j_\ell + g_1(\nu_2)a_2 + g_1(\nu_3)a_3 , \qquad \psi_{1r} = j_r - g_1(\nu_2)b_2 - g_1(\nu_3)b_3$$

$$\psi_{2\ell} = g_2(\nu_2)a_2 + g_2(\nu_3)a_3 , \qquad \psi_{2r} = g_2(\nu_2)b_2 + g_2(\nu_3)b_3$$

$$\psi_{3\ell} = g_3(\nu_2)a_2 + g_3(\nu_3)a_3 , \qquad \psi_{3r} = - g_3(\nu_2)b_2 - g_3(\nu_3)b_3$$

$$\psi_{4\ell} = g_4(\nu_2)a_2 + g_4(\nu_3)a_3 , \qquad \psi_{4r} = g_4(\nu_2)b_2 + g_4(\nu_3)b_3$$

$$\psi_{5\ell} = g_5(\nu_2)a_2 + g_5(\nu_3)a_3 , \qquad \psi_{5r} = - g_5(\nu_2)b_2 - g_5(\nu_3)b_3$$

where a_2, a_3, b_2, and b_3 are constants, ν_2 and ν_3 are the two largest positive roots of the determinental Eq. (16), and the g_n's are given by Eq. (15). From the above equations it follows that

$$(A_0 \pm B_0) = \frac{1}{2}(\phi_\ell \pm \phi_r) + \frac{1}{2}(a_2 \pm b_2)\left[1 - \frac{5}{2} g_2(\nu_2) + \frac{27}{8} g_4(\nu_2)\right]$$

$$+ \frac{1}{2}(a_3 \pm b_3)\left[1 - \frac{5}{2} g_2(\nu_3) + \frac{27}{8} g_4(\nu_3)\right]$$

$$(A_1 \mp B_1) = \frac{3}{2}(j_\ell \mp j_r) + \frac{3}{2}(a_2 \pm b_2)\left[g_1(\nu_2) - \frac{7}{2} g_3(\nu_2) + \frac{55}{8} g_5(\nu_2)\right]$$

$$+ \frac{3}{2}(a_3 \pm b_3)\left[g_1(\nu_3) - \frac{7}{2} g_3(\nu_3) + \frac{55}{8} g_5(\nu_3)\right]$$

$$(A_2 \pm B_2) = \frac{15}{4}(a_2 \pm b_2)\left[g_2(\nu_2) - \frac{9}{2} g_4(\nu_2)\right] + \frac{15}{4}(a_3 \pm b_3)\left[g_2(\nu_3) - \frac{9}{2} g_4(\nu_3)\right]$$

$$(A_3 \mp B_3) = \frac{35}{4}(a_2 \pm b_2)\left[g_3(\nu_2) - \frac{11}{2} g_5(\nu_2)\right] + \frac{35}{4}(a_3 \pm b_3)\left[g_3(\nu_3) - \frac{11}{2} g_5(\nu_3)\right]$$

$$(A_4 \pm B_4) = \frac{315}{16}(a_2 \pm b_2) g_4(\nu_2) + \frac{315}{16}(a_3 \pm b_3) g_4(\nu_3)$$

$$(A_5 \mp B_5) = \frac{693}{16}(a_2 \pm b_2) g_5(\nu_2) + \frac{693}{16}(a_3 \pm b_3) g_5(\nu_3) .$$

By adding and subtracting the matching conditions (Eqs. 5 and 6) for L = 5 one obtains:

$\underline{m = 1}$

$$(A_0 \pm B_0)\left(\frac{1}{2} - R_{10} \mp T_{10}\right) - (A_1 \mp B_1)\left(\frac{1}{3} + R_{11} \pm T_{11}\right)$$

$$+ (A_2 \pm B_2)\left(\frac{1}{4} - R_{12} \mp T_{12}\right) - (A_3 \mp B_3)\left(\frac{1}{5} + R_{13} \pm T_{13}\right)$$

$$+ (A_4 \pm B_4)\left(\frac{1}{6} - R_{14} \mp T_{14}\right) - (A_5 \mp B_5)\left(\frac{1}{7} + R_{33} \pm T_{33}\right) = 0$$

$\underline{m = 3}$

$$(A_0 \pm B_0)\left(\frac{1}{4} - R_{30} \mp T_{30}\right) - (A_1 \mp B_1)\left(\frac{1}{5} + R_{31} \pm T_{31}\right)$$

$$+ (A_2 \pm B_2)\left(\frac{1}{6} - R_{32} \mp T_{32}\right) - (A_3 \mp B_3)\left(\frac{1}{7} + R_{33} \pm T_{33}\right)$$

$$+ (A_4 \pm B_4)\left(\frac{1}{8} - R_{34} \mp T_{34}\right) - (A_5 \mp B_5)\left(\frac{1}{9} + R_{35} \pm T_{35}\right) = 0$$

$\underline{m = 5}$

$$(A_0 \pm B_0)\left(\frac{1}{6} - R_{50} \mp T_{50}\right) - (A_1 \mp B_1)\left(\frac{1}{7} + R_{51} \pm T_{51}\right)$$

$$+ (A_2 \pm B_2)\left(\frac{1}{8} - R_{52} \mp T_{52}\right) - (A_3 \mp B_3)\left(\frac{1}{9} + R_{53} \pm T_{53}\right)$$

$$+ (A_4 \pm B_4)\left(\frac{1}{10} - R_{54} \mp T_{54}\right) - (A_5 \mp B_5)\left(\frac{1}{11} + R_{55} \pm T_{55}\right) = 0$$

These three matching equations together with the previous equations for pairs of constants of the form $(A_n \pm B_n)$ determine α (upper set of signs) and β (lower set of signs) in the P_5 approximation. Although the algebra is very tedious, the three matching equations are used to eliminate the constants $(a_2 + b_2)$ and $(a_3 + b_3)$ and the resulting equation is solved for $(j_\ell - j_r)/(\phi_\ell + \phi_r)$, which is α. The blackness coefficient β is found in a similar manner or by taking the expression for α and changing the sign of all of the transmission coefficients, T_{mn}.

If we again assume linear anisotropic scattering with $\bar{\alpha} = 0$, the P_5 form of the determinental equation (Eq. 16) is

$$\begin{vmatrix} 0 & \nu & 0 & 0 & 0 & 0 \\ \nu & 3\Sigma_{tr}/\Sigma_t & 2\nu & 0 & 0 & 0 \\ 0 & 2\nu & 5 & 3\nu & 0 & 0 \\ 0 & 0 & 3\nu & 7 & 4\nu & 0 \\ 0 & 0 & 0 & 4\nu & 9 & 5\nu \\ 0 & 0 & 0 & 0 & 5\nu & 11 \end{vmatrix} = 0$$

which reduces to

$$\nu^2[225\nu^4 - 2646\nu^2 + 3465] = 0.$$

The allowed values of ν are therefore

$$\nu_i = 0,\ 0,\ \pm 1.2252109,\ \pm 3.2029453$$

and so $\nu_2 = 1.2252109$ and $\nu_3 = 3.2029453$. It follows from Eq. (15) that

$$g_1(\nu) = -\bar{\alpha}/\nu = 0$$

$$g_2(\nu) = -1/2$$

$$g_3(\nu) = 5/6\nu$$

$$g_4(\nu) = 3/8 - 35/24\nu^2$$

$$g_5(\nu) = -\frac{1}{5\nu}\left[9\, g_4(\nu) + 4\,\nu\, g_3(\nu)\right] .$$

With these constants, the methods described earlier may be used to evaluate α and β in the P_5 approximation. Like the P_3 case, α and β are independent of the properties of the external media for linear anisotropic scattering with $\bar{\alpha} = 0$.

5.5 Blackness Coefficients for a Purely Absorbing Slab

For the case of a purely absorbing slab ($\Sigma_s = 0$) all the reflection coefficients vanish, that is $R_{mn} = 0$. In Section 3 it was shown that for this special case the transmission coefficients can be expressed analytically. Thus,

$$T_{mn}\ (\Sigma_a\tau) = \int_0^1 \mu^{m+n}\ e^{-\Sigma_a\tau/\mu}\ d\mu = E_{m+n+2}\ (\Sigma_a\tau)$$

where $E_{m+n+2}\ (\Sigma_a\tau)$ is the exponential integral of order m+n+2. Using these expressions for the reflection and transmission coefficients, all the previous equations for α and β are directly applicable to the no scattering case. For example, in the P_1 approximation Eqs. (18) and (19) reduce to

$$\alpha_o = \frac{1 - 2\ E_3\ (\Sigma_a\tau)}{2\ [1 + 3\ E_4\ (\Sigma_a\tau)]} \tag{24}$$

$$\beta_o = \frac{1 + 2\ E_3\ (\Sigma_a\tau)}{2\ [1 - 3\ E_4\ (\Sigma_a\tau)]} \tag{25}$$

where the subscript on α and β serves as a reminder that these equations apply to the zero scattering case. These equations were first given by Goldsmith in Ref. 7. In a similar way the previous results can be used to obtain the P_3 and P_5 approximations for the zero scatter blackness coefficients.

5.6 The "Dirty Blackness" Approximation

For a perfectly black absorber ($\Sigma_a \to \infty$) Eqs. (24) and (25) reduce to $\alpha = \beta = 1/2$. However, from the expression for the extrapolation distance into a vacuum from a plane surface ($d = 0.7104\ \lambda_{tr}$) it is easy to show that $\alpha = 0.4692$ for this perfect absorber. Although without mathematical justification, improved values for the $\Sigma_s = 0$ blackness coefficients result if Eqs. (24) and (25) are multiplied by 0.4692/0.5. We will call these modified values "dirty blackness" (DB) coefficients and they are given by the equations

$$\alpha_o\ (DB) = 0.4692\ \frac{[1 - 2\ E_3\ (\Sigma_a\tau)]}{[1 + 3\ E_4\ (\Sigma_a\tau)]} \tag{26}$$

$$\beta_o\ (DB) = 0.4692\ \frac{[1 + 2\ E_3\ (\Sigma_a\tau)]}{[1 - 3\ E_4\ (\Sigma_a\tau)]}. \tag{27}$$

It is interesting to note that in the P_5 approximation ($\Sigma_s \neq 0$) for a very strong absorber ($\Sigma_a\tau = 15.76$) the blackness coefficients have the values $\alpha = \beta = 0.4690$. Equations (26) and (27) often give a good approximation for the blackness coefficients for those groups for which $\Sigma_s \ll \Sigma_a$. For the fast groups, where the $\Sigma_s = 0$ approximation is not valid, the absorption cross sections are small enough so that normal diffusion theory can be used and blackness theory is not needed.

6. FINE-GROUP-WEIGHTED BLACKNESS COEFFICIENTS

The weighted values of the blackness coefficients are defined by the equations

$$\langle\alpha\rangle = \frac{\langle J_\ell + J_r\rangle}{\langle\phi_\ell + \phi_r\rangle} = \frac{\int_{\Delta u} \alpha(u)[\phi_\ell(u) + \phi_r(u)]du}{\int_{\Delta u} [\phi_\ell(u) + \phi_r(u)]du} \tag{28}$$

$$\langle\beta\rangle = \frac{\langle J_\ell - J_r\rangle}{\langle\phi_\ell - \phi_r\rangle} = \frac{\int_{\Delta u} \beta(u)[\phi_\ell(u) - \phi_r(u)]du}{\int_{\Delta u} [\phi_\ell(u) - \phi_r(u)]du} \tag{29}$$

where Δu is the lethargy range of the broad group. Because the same surface flux combinations appear in both the numerator and denominator in the expressions for $\langle\alpha\rangle$ and $\langle\beta\rangle$, highly precise values of ϕ_ℓ and ϕ_r are probably not necessary. In this formalism $\alpha(u)$ and $\beta(u)$ are the fine group values of the blackness coefficients and are evaluated, usually in the P_5 approximation, by the methods discussed earlier. The fine-group surface fluxes used for weighting are determined from a one-dimensional P_1, S_8 transport calculation using a code such as ONEDANT.[2] Fine-group cross sections needed in the evaluation of $\alpha(u)$, $\beta(u)$, $\phi_\ell(u)$, and $\phi_r(u)$ were obtained from the EPRI-CELL code.[10] With this information Eqs. (28) and (29) may be numerically integrated to determine $\langle\alpha\rangle$ and $\langle\beta\rangle$ for each of the broad groups of interest. Other weighting schemes for determining $\langle\alpha\rangle$ and $\langle\beta\rangle$ have been proposed in the literature (see Ref's. 11 and 12).

It is usually sufficient to determine $\langle\alpha\rangle$ and $\langle\beta\rangle$ only for the thermal and epithermal broad groups. For the fast groups α and β can be calculated from the broad-group macroscopic cross sections. The standard five-group structure used at ANL for thermal reactor calculations and the number of fine groups corresponding to the thermal and epithermal broad groups is shown below

Standard Group Structure

Group	E_u(eV)	Number of Fine Groups
1	1.0 E+07	
2	8.208 E+05	
3	5.531 E+03	32
4	1.855	14
5	0.6249	21

7. CONTROL SLAB EFFECTIVE DIFFUSION PARAMETERS

The blackness coefficients form a pair of internal boundary conditions applicable on the surfaces of the absorber slab. However, most diffusion codes are not programmed to handle these internal boundary conditions. Therefore, it is convenient to determine effective diffusion parameters (D, Σ_a) which preserve the current-to-flux ratios on the surfaces of the control slab in terms of the blackness coefficients. Since these effective diffusion parameters are to be used in a finite difference solution, the effective constants will be expressed in such a way as to contain an explicit dependence on the mesh interval size, h. This procedure allows one to use a very coarse mesh in the absorber for the diffusion calculations.

Two cases will be considered. In the first case effective diffusion parameters will be derived for use in those diffusion codes, such as DIF3D,[8] which evaluate fluxes at the center of the mesh intervals. In the second case effective values for D and Σ_a will be obtained for use in diffusion codes which evaluate fluxes on the mesh interval boundaries.

7.1 Case for Mesh-Centered Fluxes

For the purpose of this derivation, it is convenient to assume that the same material extends to regions outside the absorber slab of thickness τ. Since α and β depend only on the properties inside the slab, this assumption leads to no loss in generality. One first needs to find the surface flux and current ϕ_ℓ and J_ℓ, in terms of the mesh-centered fluxes ϕ_1 and ϕ_{-1} (see figure).

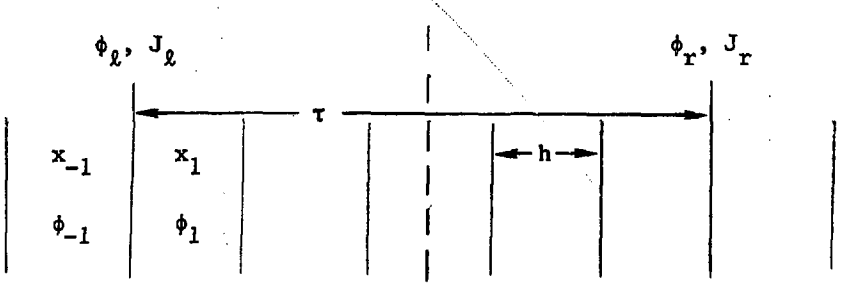

Control Slab

Assuming that the flux varies linearly from the edge to the center of the mesh cell, it follows that

$$\phi_1 = \phi_\ell + \frac{h}{2}\phi_\ell' = \phi_\ell - \frac{h}{2D} J_\ell$$

$$\phi_{-1} = \phi_\ell - \frac{h}{2}\phi_\ell' = \phi_\ell + \frac{h}{2D} J_\ell$$

where h is the width of the mesh interval. Thus,

$$\phi_\ell = \frac{1}{2}(\phi_{-1} + \phi_1)$$

$$J_\ell = \frac{D}{h}(\phi_{-1} - \phi_1)$$

It is convenient to consider symmetric and asymmetric solutions to the diffusion equation separately.

Symmetric Solution

For this case $J_\ell = J_r$ and $\phi_\ell = \phi_r$ so that

$$\alpha = \frac{J_\ell + J_r}{\phi_\ell + \phi_r} = \frac{J_\ell}{\phi_\ell} = \frac{2D}{h}\frac{(\phi_{-1} - \phi_1)}{(\phi_{-1} + \phi_1)}$$

where

$$\phi_1 = C \cosh kx_1 = C \cosh \frac{k}{2}(\tau - h)$$

$$\phi_{-1} = C \cosh kx_{-1} = C \cosh \frac{k}{2}(\tau + h)$$

and where x is measured from the center of the slab. After some manipulation, the expression for α becomes

$$\alpha = \frac{2D}{h}[\sinh(k\tau/2)\sinh(kh/2)]/[\cosh(k\tau/2)\cosh(kh/2)]$$

Asymmetric Solution

For this case $J_\ell = -J_r$ and $\phi_\ell = -\phi_r$ so that

$$\beta = \frac{J_\ell - J_r}{\phi_\ell - \phi_r} = \frac{J_\ell}{\phi_\ell} = \frac{2D}{h}\frac{(\phi_{-1} - \phi_1)}{(\phi_{-1} + \phi_1)}$$

where now

$$\phi_1 = A \sinh kx_1 = A \sinh \frac{k}{2}(\tau - h)$$

$$\phi_{-1} = A \sinh kx_{-1} = A \sinh \frac{k}{2}(\tau + h)$$

The expression for β reduces to

$$\beta = \frac{2D}{h} [\cosh (k\tau/2) \sinh (kh/2)]/[\sinh (k\tau/2) \cosh (kh/2)].$$

Thus,

$$\frac{\alpha}{\beta} = \frac{\tanh (k\tau/2)}{\coth (k\tau/2)} = \tanh^2 (k\tau/2).$$

This equation determines k in terms of α and β. It can be put into a more useful form by making use of the identity

$$\tanh^{-1}x = \frac{1}{2} \ln\left[\frac{1 + x}{1 - x}\right] \qquad \text{Hence,}$$

$$k = \frac{1}{\tau} \ln \left[\frac{\beta^{1/2} + \alpha^{1/2}}{\beta^{1/2} - \alpha^{1/2}}\right] . \tag{30}$$

By adding the above equations for α and β it can be shown that

$$D = \frac{h}{2} (\alpha + \beta) \frac{\tanh k\tau}{\sinh kh} [\frac{1}{2} (1 + \cosh kh)] . \tag{31}$$

An expression for Σ_a can be obtained from the diffusion equation written in the difference form and solving for Σ_a. Thus,

$$\Sigma_a = \frac{D}{h^2} \left[\frac{\phi_{n+1}}{\phi_n} - 2 + \frac{\phi_{n-1}}{\phi_n}\right].$$

By substituting

$$\phi_n = C \cosh kx_n$$

$$\phi_{n+1} = C \cosh k(x_n + h) = C[\cosh kx_n \cosh kh + \sinh kx_n \sinh kh]$$

$$\phi_{n-1} = C \cosh k(x_n - h) = C[\cosh kx_n \cosh kh - \sinh kx_n \sinh kh]$$

into the above equation it follows that

$$\Sigma_a = \frac{2D}{h^2} [\cosh kh - 1] . \tag{32}$$

Note that this equation is valid for both mesh-centered and mesh-boundary fluxes.

Equations (30-32) determine the effective diffusion parameters in terms of the blackness coefficients. Since these equations incorporate h explicitly, a very coarse mesh may be used. The equations are applicable for the case where the diffusion code determines fluxes at the center of mesh intervals.

Diffusion parameters can be obtained to describe the behavior of an effectively black absorber. For this limiting case $\alpha \to \beta \to 0.4692$ and k_τ (Eq. 30) tends to infinity. It is sufficient to set k_τ equal to an arbitarily large, but finite, value such as $k_\tau = 10$. For a black absorber Eq. (31) reduces to

$$D \to h\,\alpha/2 = 0.2346\ h\ .$$

And Eq. (32) becomes

$$\Sigma_a \to \frac{0.4692}{h}\ e^{10}\ .$$

This is equivalent to using a black internal boundary ($j/\phi = 0.4692$) in the DIF3D[8] code.

7.2 Case for Mesh-Boundary Fluxes

The same general procedures may be used to derive effective diffusion parameters for the case where fluxes are evaluated on the boundaries of the mesh intervals. Written in finite difference form, the diffusion equation and Fick's law become

$$\frac{\phi_{n+1} - 2\phi_n + \phi_{n-1}}{h^2} - k^2\,\phi_n = 0$$

$$j_n = -\frac{D}{2h}\,(\phi_{n+1} - \phi_{n-1})\ .$$

Again for the purpose of the derivation, we assume that the same material extends to regions outside the absorber slab of thickness τ only now the fluxes are specified on the mesh boundaries. It follows from the above equations and Eq. (32) that

$$\phi_\ell = \frac{1}{2}\,(\phi_{-1} + \phi_1)/(1 + \frac{1}{2}\,k^2h^2) = \frac{1}{2}\,(\phi_{-1} + \phi_1)/\cosh kh$$

$$J_\ell = j_\ell = \frac{D}{2h}\,(\phi_{-1} - \phi_1)\ .$$

As before, we consider separately symmetric and asymmetric solutions to the diffusion equation.

Symmetric Solution

For this case $J_\ell = J_r$ and $\phi_\ell = \phi_r$ so that

$$\alpha = \frac{J_\ell + J_r}{\phi_\ell + \phi_r} = \frac{J_\ell}{\phi_\ell} = \frac{D}{h}\ \frac{(\phi_{-1} - \phi_1)}{(\phi_{-1} + \phi_1)}\ \cosh kh$$

where

$$\phi_1 = C \cosh kx_1 = C \cosh k\,(\tau/2 - h)$$

$$\phi_{-1} = C \cosh kx_{-1} = C \cosh k\,(\tau/2 + h)$$

Substituting these fluxes into the equation for α and simplifying one obtains

$$\alpha = \frac{D}{h} \sinh kh \tanh k\tau/2 \quad .$$

Asymmetric Solution

For this case $J_\ell = -J_r$ and $\phi_\ell = -\phi_r$ so that

$$\beta = \frac{J_\ell - J_r}{\phi_\ell - \phi_r} = \frac{J_\ell}{\phi_\ell} = \frac{D}{h} \frac{(\phi_{-1} - \phi_1)}{(\phi_{-1} + \phi_1)} \cosh kh$$

where now

$$\phi_1 = A \sinh kx_1 = A \sinh k\,(\tau/2 - h)$$

$$\phi_{-1} = A \sinh kx_{-1} = A \sinh k\,(\tau/2 + h)$$

Substituting these fluxes into the expression for β and simplifying, it follows that

$$\beta = \frac{D}{h} \sinh kh \coth k\tau/2 \quad .$$

Hence,

$$\frac{\alpha}{\beta} = \tanh^2 (k\tau/2) \quad .$$

This is the same result as that obtained in pararaph 7.1. Therefore,

$$k = \frac{1}{\tau} \ln \left[\frac{\beta^{1/2} + \alpha^{1/2}}{\beta^{1/2} - \alpha^{1/2}} \right] .$$

By adding the above equations for α and β it follows that

$$D = \frac{h}{2} (\alpha + \beta) \frac{\tanh k\tau}{\sinh kh} \quad . \tag{33}$$

We see that Eqs. (30) and (32) also apply to the case where fluxes are calculated on the mesh boundaries and that only the expression for the diffusion coefficient [compare Eqs. (31) and (33)] changes.

For the limit of a black absorber, $D \to 0$ and $\Sigma_a \to 2\alpha/h = 0.9384/h$. Setting $k\tau = 10$ in Eq. (33) will yield results essentially indistinguishable from the limiting case.

7.3 Verification

The effective diffusion parameters were chosen so as to preserve the values of the blackness coefficients on the surfaces of the control slab. To verify that this has been accomplished, fluxes from the diffusion calculation can be used to evaluate ϕ_ℓ, J_ℓ, ϕ_r, and J_r which determine α and β. Using procedures similar to those described in the first part of paragraph 7.1, it is easy to show that for mesh-centered fluxes

$$\phi_\ell = \frac{\frac{D_o}{h_o}\phi_o + \frac{D_i}{h_i}\phi_i}{\frac{D_o}{h_o} + \frac{D_i}{h_i}}, \quad J_\ell = \frac{2(\phi_o - \phi_i)}{(\frac{h_o}{D_o} + \frac{h_i}{D_i})} \tag{34}$$

where ϕ_o and ϕ_i are the fluxes just outside and just inside the left-hand surface of the absorber slab. D_o, D_i, h_o, and h_i are the diffusion coefficients and mesh intervals on each side of the left-hand surface of the absorber slab. Similar equations are used to evaluate ϕ_r and J_r on the right-hand surface. Then,

$$\alpha = \frac{J_\ell + J_r}{\phi_\ell + \phi_r} \qquad \text{and} \qquad \beta = \frac{J_\ell - J_r}{\phi_\ell - \phi_r}$$

and these values based on the fluxes from the diffusion code should be the same as those used to determine the effective diffusion parameters.

For diffusion codes which evaluate fluxes on the mesh interval boundaries, ϕ_ℓ and ϕ_r are given in the output of the problem and

$$J_\ell = \frac{(\phi_o - \phi_i)}{\left(\frac{h_o}{D_o} + \frac{h_i}{D_i}\right)} \tag{35}$$

with a similar equation for J_r. As before, α and β may be calculated from these surface fluxes and currents and compared with those used to calculate the effective diffusion parameters.

8. PROCEDURE FOR CALCULATING BLACKNESS COEFFICIENTS AND THE CORRESPONDING EFFECTIVE DIFFUSION PARAMETERS

In the previous sections the formalism was developed for determining α and β and the corresponding values of D and Σ_a for the control slab. A procedure for calculating the numerical values of these constants is outlined in the steps below.

1. The EPRI-CELL Code[10] is used to generate both broad and fine group cross sections for the control material, its immediate environment, and the fuel region. Because of code limitations, two cross section sets having different group structures are generated. The first set consists of two fast groups, 32 epithermal fine groups and two broad thermal groups for a total of 36 groups. The second set consists of two fast and one epithermal broad groups and 35 thermal fine groups for a total of 38 groups. Energy boundaries for the fine groups are just those used in the EPRI-CELL input cross section library. A brief outline of the group structure is given at the end of Section 6. For control materials having large low energy resonances, such as Ag, In, and Hf, it may be necessary to generate the fine-group epithermal cross sections with the MC^2-2 Code.[13] The RABANL module of MC^2-2 rigorously treats resolved resonance absorption whereas EPRI-CELL does not.

2. Using the ONEDANT Code[2] together with the EPRI-CELL cross sections, 1D transport calculations (P_1, S_8) are performed to determine the absorber surface fluxes needed for weighting the fine-group blackness coefficients. These surface fluxes are saved on a file for later use. The file of macroscopic cross sections for the control slab is also saved. Because of the strongly absorbing character of the control slab, a fine mesh structure is needed, especially near the surfaces of the slab. For some calculations mesh intervals near the slab surfaces of less than 0.001 cm have been used.

3. With the file of the control slab fine-group macroscopic cross sections Σ_a, Σ_t, and Σ_s, a series of ONEDANT source calculations (P_1, S_{24}) are performed to determine the angular flux distribution on the surfaces of the slab. With a source distribution of the form μ^n, six calculations are needed corresponding to n = 0, 1, 2, 3, 4, 5. A program has been written to calculate and store the reflection and transmission coefficients, R_{mn} and T_{mn}, from the ONEDANT angular flux file. Since these coefficients will be used to calculate the blackness coefficients in the P_5 approximation, m values (See Eqs. 1 and 2) of 1, 3, and 5 are needed. For 67 fine groups and 5 broad groups a total of 1296 reflection coefficients and an equal number of transmission coefficients are calculated.

4. The file of reflection and transmission coefficients is used in another program to calculate the fine-group and broad-group blackness coefficients in the P_1, P_3, P_5 and no-scatter approximations. Using the file of surface fluxes, the program also calculates the fine-group-weighted blackness coefficients, $\langle\alpha\rangle$ and $\langle\beta\rangle$. Finally, these values are used to determine the broad-group effective diffusion parameters D and Σ_a. These parameters are calculated for mesh intervals corresponding to $h = \tau/n$ with n = 1, 2, 3, 4, and 5.

5. Control rod worths are evaluated using diffusion theory with these modified macroscopic cross sections for the control material.

9. APPLICATIONS

In this section the blackness coefficients and the corresponding effective diffusion parameters are evaluated for several types of control elements using the methods discussed earlier. Eigenvalues based on this blackness-modified diffusion theory are compared with those obtained from continuous-energy Monte Carlo methods.

9.1 Cadmium Control Elements

Control elements for the 30-MW Oak Ridge Research Reactor (ORR) consist of square, water-filled cadmium boxes 5.8912 cm on a side and 77.47 cm long. The boxes are formed from a sheet of natural cadmium 0.1016 cm thick and clad in 0.0508 cm thick aluminum.

Fine-group cross sections were generated by the EPRI-CELL Code.[10] Reflection and transmission coefficients for each of the fine groups were obtained by numerically integrating Eqs. (1) and (2) using ONEDANT[2] values for the surface angular fluxes, $\psi_n(0,\mu)$ and $\psi_n(\tau,\mu)$. Using the methods described in Section 5, fine-group blackness coefficients were evaluated from the reflection and transmission coefficients in various orders of approximation. Broad-group blackness coefficients, $\langle\alpha\rangle$ and $\langle\beta\rangle$, were obtained by weighting the fine-group values as described in Section 6.

Results for the broad-group blackness coefficients, calculated in the P_1, P_3, and P_5 approximations and by "dirty blackness" theory, are summarized in Table III. Fick's law is valid provided the second derivative of the flux does not change significantly over a few mean free paths within the absorber. Thus, diffusion theory should be valid for those groups for which $\Sigma_a \ll \Sigma_s$. Table III shows that blackness theory is really needed only for groups 4 and 5. Even group 4 could be treated with diffusion theory with little loss in accuracy because of the narrowness of this group and because $\tau/L \ll 1$ for group-4 neutrons, where L is the diffusion length in the absorber slab. "Dirty blackness" theory gives remarkably good results for the group-5 blackness coefficients, as Table III indicates. However, Eqs. (24) and (25) were derived for the case of no scattering. As scattering within the slab becomes significant, the "dirty blackness" coefficients, especially β, become progressively worse, as Table III shows. Note that for a black absorber $\alpha = \beta = 0.4692$. Thus, the cadmium is nearly black to group-5 neutrons.

The effective diffusion parameters corresponding to the broad-group blackness coefficients were calculated from Eqs. (30-32) and are therefore applicable for use in the DIF3D Code,[8] which evaluates fluxes at the center of mesh intervals. Results from these calculations are summarized in Table IV. They apply for mesh interval spacings of $h = \tau$, $\tau/2$, $\tau/3$ and $\tau/4$.

These effective diffusion parameters, for $h = \tau/2$, were applied to the 1D and 2D models shown in Figs. 1 and 2. The fuel cross sections used in these calculations were generated for an ORR standard 19-plate element with 285 g ^{235}U. Eigenvalues obtained from blackness-modified diffusion theory are compared with those from VIM[14]/Monte Carlo calculations in Table V. Note that eigenvalues obtained by using normal diffusion theory in the cadmium region for groups 1-4 and a black internal boundary condition ($j/\phi = 0.4692$) for group 5 are in good agreement with those based on the use of effective diffusion parameters, as one would expect.

Table III. Broad-Group Blackness Coefficients for a 0.1016-cm-Thick Cadmium Slab.

Quantity	Group 1	Group 2	Group 3	Group 4	Group 5
E_u (eV)	1.0E+07	8.208E+05	5.531E+03	1.855	0.6249
Σ_a/Σ_s	5.7044E-03	3.5980E-02	4.6885E-01	3.3797	2.7866E+02
$\Sigma_a\tau$	1.4074E-04	1.1472E-03	1.6371E-02	8.3122E-02	6.8515E+00
No. of Fine Groups	1	1	32	14	21
$\alpha(P_1)$	7.2308E-05	5.7402E-04	8.0056E-03	3.8072E-02	4.9904E-01
$\alpha(P_3)$	7.2304E-05	5.7374E-04	7.9567E-03	3.7158E-02	4.7188E-01
$\alpha(P_5)$	7.2304E-05	5.7371E-04	7.9516E-03	3.7084E-02	4.6980E-01
$\langle\alpha(P_5)\rangle$	7.2304E-05	5.7371E-04	7.0560E-03	3.6251E-02	4.4449E-01
$\langle\alpha(DB)\rangle$*	6.9793E-05	5.6720E-04	6.6565E-03	3.4987E-02	4.4366E-01
$\beta(P_1)$	2.6866E+01	2.0183E+01	1.3004E+01	6.2150E+00	4.9955E-01
$\beta(P_3)$	2.6868E+01	2.0183E+01	1.3002E+01	6.2058E+00	4.7241E-01
$\beta(P_5)$	2.6868E+01	2.0183E+01	1.3002E+01	6.2041E+00	4.7035E-01
$\langle\beta(P_5)\rangle$	2.6868E+01	2.0183E+01	1.3453E+01	8.6247E+00	4.7099E-01
$\langle\beta(DB)\rangle$*	4.7010E+03	5.7673E+02	1.9728E+03	1.4705E+01	4.6982E-01

*Weighted Average of the "dirty blackness" coefficients (see Eqs. 26 and 27).

Table IV. Cadmium P_5 Effective Diffusion Parameters for Mesh-Centered Fluxes with Fine-Group-Weighted α and β.

Group	$\langle\alpha\rangle$	$\langle\beta\rangle$	k	D_{eff}	Σ_{tr}	$\Sigma_{a_{eff}}$	h(cm)
1	7.23039D-05	2.68679D+01	3.22925D-02	1.36489D+00	2.44220D-01	1.42331D-03	$h=\tau=1.01600D-01$
2	5.73709D-04	2.01829D+01	1.04953D-01	1.02529D+00	3.25111D-01	1.12938D-02	"
3	7.05597D-03	1.34533D+01	4.50896D-01	6.83426D-01	4.87739D-01	1.38970D-01	"
4	3.62513D-02	8.62472D+00	1.27801D+00	4.38136D-01	7.60799D-01	7.16621D-01	"
5	4.44494D-01	4.70986D-01	4.16884D+01	2.39261D-02	1.39318D+01	1.55559D+02	"
1	7.23039D-05	2.68679D+01	3.22925D-02	1.36489D+00	2.44221D-01	1.42331D-03	$h=\tau/2=5.08000D-02$
2	5.73709D-04	2.01829D+01	1.04953D-01	1.02528D+00	3.25113D-01	1.12936D-02	"
3	7.05597D-03	1.34533+01	4.50896D-01	6.83336D-01	4.87803D-01	1.38933D-01	"
4	3.62513D-02	8.62472D+00	1.27801D+00	4.37675D-01	7.61600D-01	7.15113D-01	"
5	4.44494D-01	4.70986D-01	4.16884D+01	1.48003D-02	2.25221D+01	3.68934D+01	"
1	7.23039D-05	2.68679D+01	3.22925D-02	1.36489D+00	2.44221D-01	1.42331D-03	$h=\tau/3=3.38667D-02$
2	5.73709D-04	2.01829D+01	1.04953D-01	1.02528D+00	3.25114D-01	1.12936D-02	"
3	7.05597D-03	1.34533D+01	4.50896D-01	6.83319D-01	4.87815D-01	1.38927D-01	"
4	3.62513D-02	8.62472D+00	1.27801D+00	4.37590D-01	7.61749D-01	7.14834D-01	"
5	4.44494D-01	4.70986D-01	4.16884D+01	1.27407D-02	2.61628D+01	2.60738D+01	"
1	7.23039D-05	2.68679D+01	3.22925D-02	1.36489D+00	2.44221D-01	1.42331D-03	$h=\tau/4=2.54000D-02$
2	5.73709D-04	2.01829D+01	1.04953D-01	1.02528D+00	3.25114D-01	1.12936D-02	"
3	7.05597D-03	1.34533D+01	4.50896D-01	6.83314D-01	4.87819D-01	1.38924D-01	"
4	3.62513D-02	8.62472D+00	1.27801D+00	4.37560D-01	7.61801D-01	7.14737D-01	"
5	4.44494D-01	4.70986D-01	4.16884D+01	1.19823D-02	2.78189D+01	2.28442D+01	"

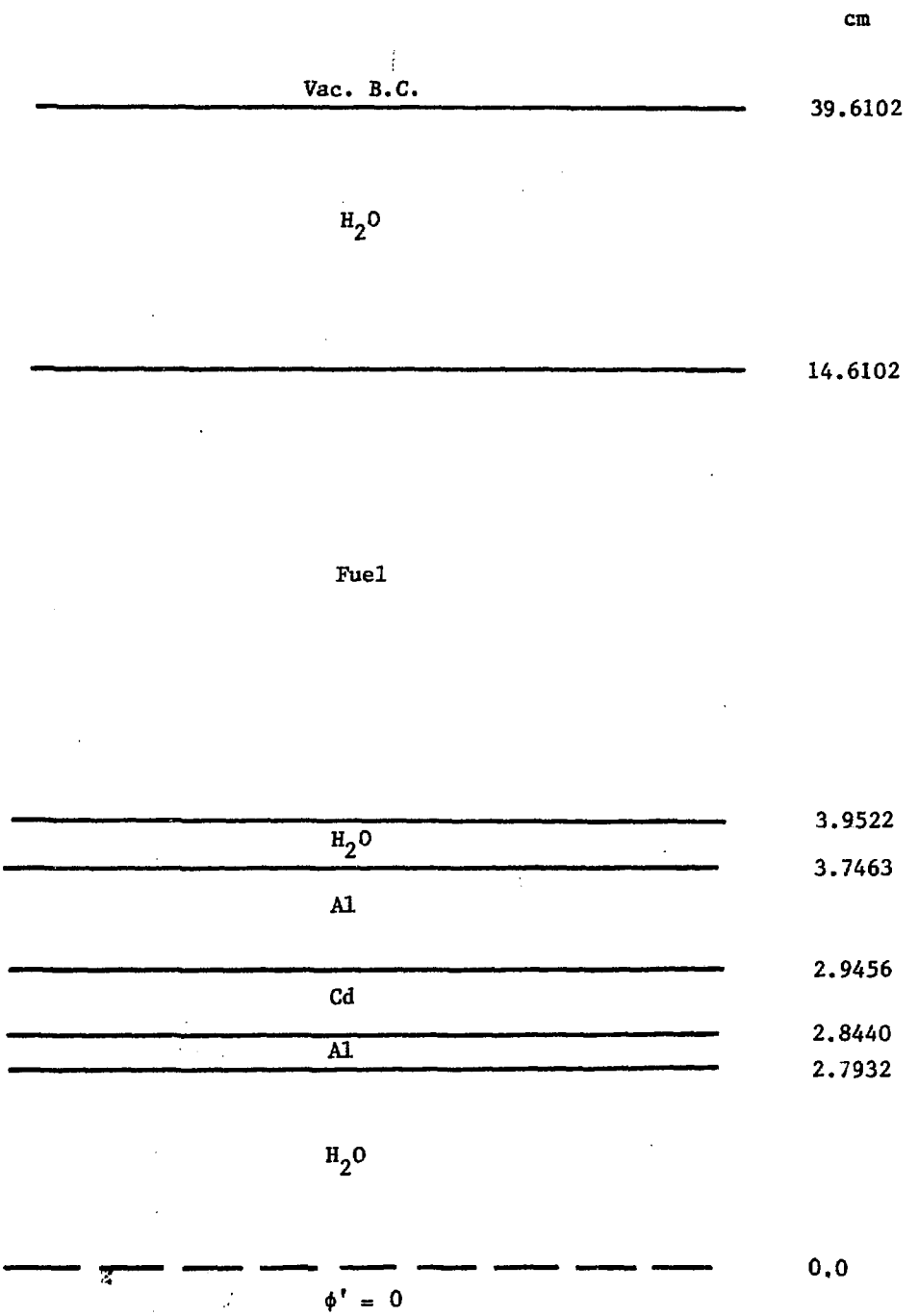

Fig. 1. Cadmium Slab Model

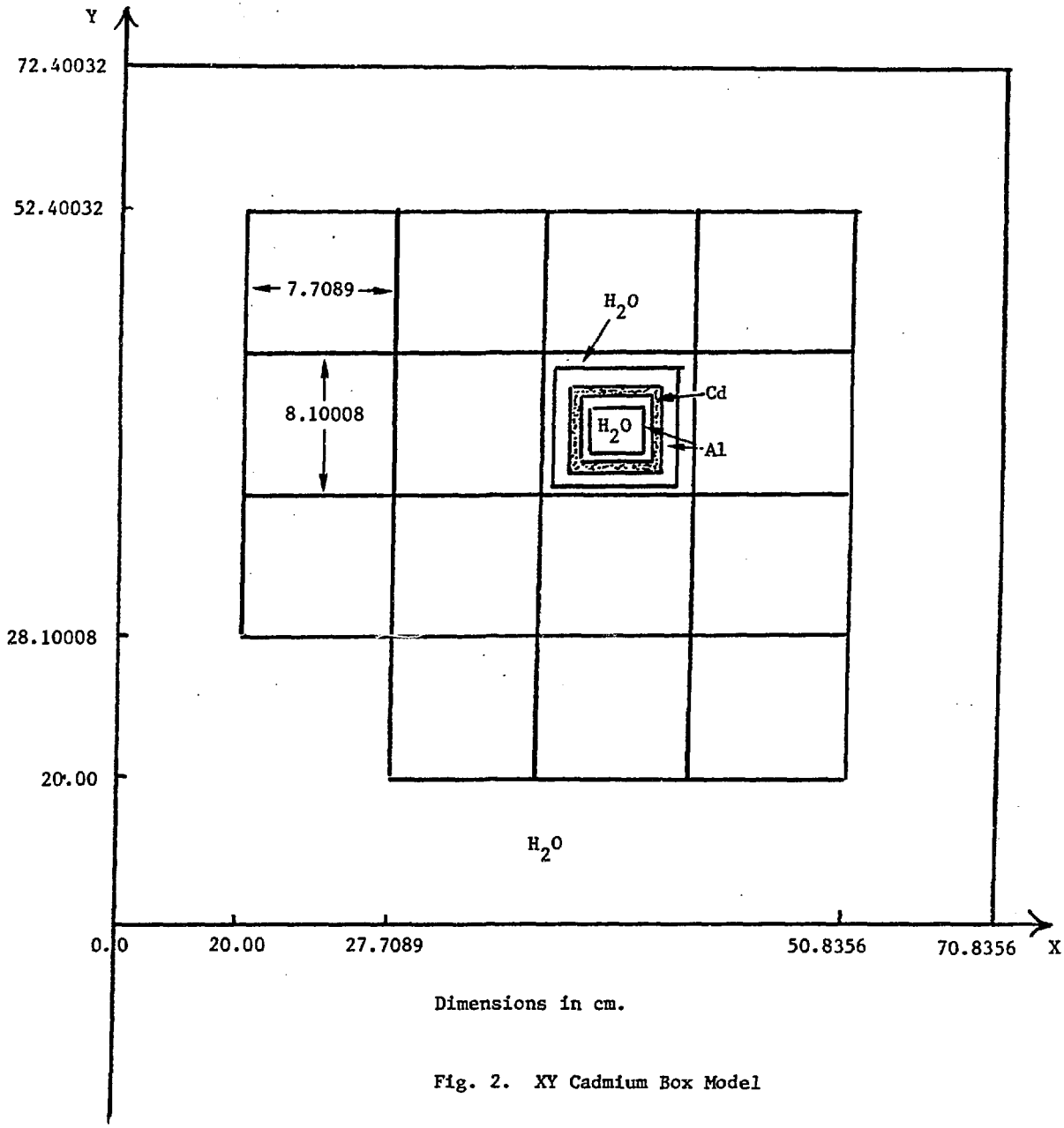

Dimensions in cm.

Fig. 2. XY Cadmium Box Model

Table V. Cadmium Rod Worths

Model	Code	Rod In k_{eff}	Rod Out k_{eff}	$\Delta\rho^*$ %
X-Slab (Fig. 1)	VIM	0.9864±0.0036	1.2291±0.0046	20.02±0.48
"	DIF3D (α,β)	0.9897	1.2290	19.67
"	DIF3D (Gp. 5 Black)	0.9870	1.2290	19.95
XY-Box (Fig. 2)	VIM	1.1380±0.0033	1.2082±0.0032	5.10±0.34
"	DIF3D (α,β)	1.1271	1.2090	6.01
"	DIF3D (Gp. 5 Black)	1.1258	1.2090	6.11
XYZ (Fig. 3)	VIM	0.9700±0.0022	1.1662±0.0025	17.34±0.30
"	DIF3D (Gp. 5 Black)	0.9654	1.1602	17.39

*$\Delta\rho \equiv (k_{out} - k_{in})/k_{out}\ k_{in}$.

The effective diffusion parameters are chosen so that the currents and fluxes on the surfaces of the absorber slab preserve the values of the blackness coefficients. To verify that this has been accomplished, the output fluxes from the one-dimensional DIF3D calculation were used to determine ϕ_ℓ, J_ℓ, ϕ_r, and J_r from Eqs. (34) and α and β from Eqs. (8) and (9). The results for group-5 neutrons are shown below.

Quantity	Left Surface	Right Surface
h_o (cm)	0.1016	0.1016
h_i (cm)	0.0508	0.0508
D_o (cm)	3.5573	3.6509
D_i (cm)	0.0148	0.0148
ϕ_o	1.8084E+10	8.2218E+09
ϕ_i	4.0622E+09	2.1728E+09
	ϕ_ℓ = 1.8073E+10	ϕ_r = 8.2169E+09
	J_ℓ = 8.1637E+09	J_r = 3.5218E+09

Hence,

$$\alpha = \frac{J_\ell + J_r}{\phi_\ell + \phi_r} = 0.44449, \qquad \beta = \frac{J_\ell - J_r}{\phi_\ell - \phi_r} = 0.47099$$

These results are identical to $\langle\alpha(P_5)\rangle$ and $\langle\beta(P_5)\rangle$ for group-5 neutrons in Table III, which verifies that the effective diffusion parameters (Eqs. 30-32) have been properly determined.

Figure 3 shows a model of the Swedish R2 Reactor which has the same type of Cd box control elements as the ORR. Eigenvalues for an XYZ model of this reactor were obtained for various control rod configurations. The results are summarized in Table VI and in the last part of Table V and are compared with VIM[14]/Monte Carlo calculations. Withdrawn rods are in the upper reflector, and fuel followers are in the lower reflector for the inserted rods. For these calculations, group 5 was made black and groups 1-4 were treated with normal diffusion theory.

Generally speaking, Tables V and VI show that the worths of the cadmium control elements based on blackness-modified diffusion theory are in good agreement with the results of detailed Monte Carlo calculations. However, the comparison is somewhat disappointing for the XY model. No explanation for this discrepancy has been found.

9.2 Ag-In-Cd Control Elements

A number of research reactors use control elements consisting of flat blades composed of a Ag-In-Cd alloy. For the purpose of these calculations, the control blades were assumed to be 0.310 cm thick with a density of 9.32 g/cm^3 and a composition of 4.9 wt% Cd, 80.5 wt% Ag, and 14.6 wt% In. Table VII shows the broad-group blackness coefficients for the 0.31-cm-thick Ag-In-Cd slab calculated by the procedures outlined in Section 8. The values of the Σ_a/Σ_s ratios given in Table VII show that normal diffusion theory could be used for groups 1 and 2 whereas blackness theory is needed for

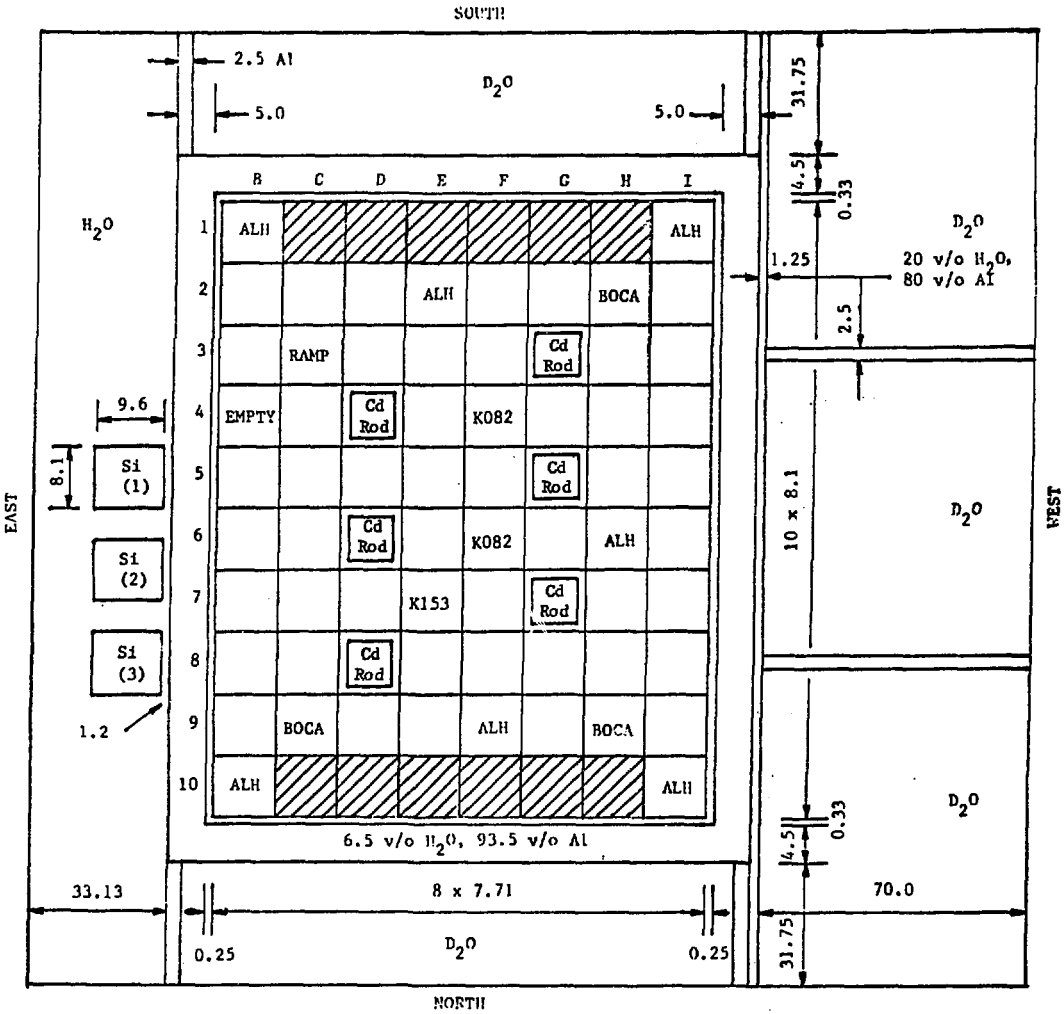

Fig. 3. The R2 Reactor Model.

Table VI. Eigenvalues and Cadmium Control Rod Worths for the Swedish R2 Reactor.

Fuel[a]	Rod Config.	k_{eff} DIF3D[b]	$\Delta\rho$[c] %	k_{eff} VIM	$\Delta\rho$[c] %
HEU 25019	All Out	1.1602		1.1662±0.0025	
"	All In	0.9654	17.39	0.9700±0.0022	17.34±0.30
"	At 50%	1.0826	6.18	1.0862±0.0024	6.32±0.27
"	Only G3 Out	1.0233	11.53	1.0266±0.0024	11.66±0.29
LEU 32618	All Out	1.1562		1.1537±0.0020	
"	All In	0.9655	17.09	0.9656±0.0025	16.89±0.31
"	At 50%	1.0816	5.97	1.0790±0.0026	6.00±0.27
"	Only G3 Out	1.0184	11.70	1.0191±0.0025	11.45±0.28

[a]The HEU 25019 notation stands for HEU fuel with 250 g ^{235}U per 19-plate element.

[b]The DIF3D calculations were done for group 5 of cadmium made black.

[c]$\Delta\rho \equiv (k_{out} - k_{in})/k_{out}k_{in}$.

Table VII. Broad-Group Blackness Coefficients for a 0.31-cm-Thick Ag-In-Cd Slab.

Quantity	Group 1	Group 2	Group 3	Group 4	Group 5
E_u (eV)	1.0E+07	8.208E+05	5.531E+03	1.855	0.6249
Σ_a/Σ_s	0.01388	0.06620	0.9549	9.2358	14.916
$\Sigma_a\tau$	1.1788E-03	8.3250E-03	1.8357E-01	1.2372	2.0308
No. of Fine Groups	1	1	32	14	21
$\alpha(P_1)$	5.8971E-04	4.1294E-03	8.0743E-02	3.5099E-01	4.3407E-01
$\alpha(P_3)$	5.8948E-04	4.1191E-03	7.8255E-02	3.2980E-01	4.0888E-01
$\alpha(P_5)$	5.8946E-04	4.1184E-03	7.8052E-02	3.2762E-01	4.0657E-01
$\langle\alpha(P_5)\rangle$	5.8946E-04	4.1184E-03	5.3232E-02	3.0963E-01	3.8747E-01
$\langle\alpha(DB)\rangle$*	5.5110E-04	3.8370-03	5.2921E-02	3.0990E-01	3.9047E-01
$\beta(P_1)$	7.7410	4.9746	1.8153	6.6227E-01	5.4799E-01
$\beta(P_3)$	7.7410	4.9738	1.8052	6.3920E-01	5.2324E-01
$\beta(P_5)$	7.7410	4.9736	1.8037	6.3730E-01	5.2151E-01
$\langle\beta(P_5)\rangle$	7.7410	4.9736	2.4627	7.1679E-01	5.4003E-01
$\langle\beta(DB)\rangle$*	5.3069E+02	7.5151E+01	8.2595	7.8897E-01	5.6342E-01

*Weighted average of the "dirty blackness" (DB) coefficients (see Eqs. 26 and 27).

groups 3, 4, and 5. "Dirty blackness" coefficients provide a good approximation for the thermal groups, but the group-3 value of $\langle\beta(DB)\rangle$ is a poor approximation because the no-scatter condition is badly violated. Effective diffusion parameters were calculated from the values of $\langle\alpha(P_5)\rangle$ and $\langle\beta(P_5)\rangle$ using Eqs. 30-32. These parameters are given in Table VIII for the mesh intervals $h = \tau$, $\tau/2$, $\tau/3$, and $\tau/4$.

Figures 4 and 5 show one-dimensional reactor models of asymmetric and symmetric control blade positions. For these cases eigenvalues calculated by blackness-modified diffusion theory are compared with those from corresponding P_1, S_8 transport calculations. The results of this comparison are summarized in Table IX, which shows that blackness theory and transport theory yield nearly identical results. The table also shows that the mesh-dependent effective diffusion parameters produce eigenvalues independent of the number of mesh intervals in the Ag-In-Cd control blade.

The internal boundary condition option of the DIF3D Code[8] assumes that the surface currents and fluxes are the same on each side of the control blade. This condition is met only for the symmetric model (Fig. 5). Table IX shows that the internal boundary condition option of DIF3D yields results consistent with transport theory only for the symmetric case, as one would expect.

The effective diffusion parameters are chosen so as to preserve the values of the blackness coefficients on the surfaces of the control slab. To verify that this has been accomplished, DIF3D fluxes from the asymmetric model with $h = \tau/2$ were used to calculate ϕ_ℓ, J_ℓ, ϕ_r, and J_r from Eqs. (34). Table X compares the blackness coefficients calculated from these fluxes and currents with those used to determine the effective diffusion parameters. It is seen that the results are entirely consistent, showing that the effective diffusion parameters are correctly defined by Eqs. (30), (31) and (32).

The above results show that blackness theory applied to Ag-In-Cd blades in slab geometry produces very acceptable results. The method is now applied to a 3D reactor model. Figure 6 shows the locations of the forked Ag-In-Cd control blades in the 10-MW Generic Reactor.[15] Calculations were performed for the case of fresh U_3Si_2-Al LEU fuel (390 g ^{235}U per 23-plate fuel element) using both the DIF3D[8]-XYZ and VIM[14]/Monte Carlo Codes.

The blackness coefficients given in Table VII were calculated using EPRI-CELL cross sections. Because of code limitations, however, self-shielding in the low-energy resolved resonances of the Ag and In isotopes is not adequately accounted for by EPRI-CELL. Therefore, the blackness coefficients were normalized to the VIM broad-group Ag-In-Cd macroscopic cross sections by multiplying $\langle\alpha(P_5)\rangle$ by $\alpha(VIM)/\alpha(E\text{-}CELL)$ and $\langle\beta(P_5)\rangle$ by $\beta(VIM)/\beta(E\text{-}CELL)$. This normalization resulted in about a 0.5% increase in the eigenvalue. The normalization would not have been necessary if the MC^2-2 Code[13] had been used to generate the epithermal fine-group Ag-In-Cd cross sections. The RABANL module of MC^2-2 performs a hyper-fine-group integral transport slowing down calculation which rigorously treats resolved resonance absorption.

Eigenvalues from the 3D (see Fig. 6) calculations are compared in Table XI. The results show that the XYZ diffusion-theory calculations using blackness-modified diffusion parameters for the control blades agree very well with the VIM/Monte Carlo calculations.

Table VIII. Ag-In-Cd P_5 Effective Diffusion Parameters for Mesh-Centered Fluxes with Fine-Group-Weighted α and β.

Group	$\langle\alpha\rangle$	$\langle\beta\rangle$	k	D_{eff}	Σ_{tr}	$\Sigma_{a_{eff}}$	h(cm)
1	5.89456D-04	7.74088D+00	5.63002D-02	1.19984D+00	2.77816D-01	3.80323D-03	$h=\tau=3.10000D-01$
2	4.11835D-03	4.97364D+00	1.85700D-01	7.70914D-01	4.32387D-01	2.65920D-02	"
3	5.32323D-02	2.46267D+00	9.55458D-01	3.81714D-01	8.73254D-01	3.51022D-01	"
4	3.09634D-01	7.16793D-01	5.08354D+00	1.11103D-01	3.00022D+00	3.51680D+00	"
5	3.87471D-01	5.40029D-01	8.03533D+00	8.37045D-02	3.982260D+00	8.84890D+00	"
1	5.89456D-04	7.74088D+00	5.63002D-02	1.19981D+00	2.77821D-01	3.80309D-03	$h=\tau/2=1.55000D-01$
2	4.11835D-03	4.97364D+00	1.85700D-01	7.70754D-01	4.32477D-01	2.65810D-02	"
3	5.32323D-02	2.46267D+00	9.55458D-01	3.79640D-01	8.78025D-01	3.47207D-01	"
4	3.09634D-01	7.16793D-01	5.08354D+00	9.74193D-02	3.42164D+00	2.65053D+00	"
5	3.87471D-01	5.40029D-01	8.03633D+00	6.40970D-02	5.20045D+00	4.703250+00	"
1	5.89456D-04	7.74088D+00	5.63002D-02	1.19981D+00	2.77822D-01	3.80306D-03	$h=\tau/3=1.03333D-01$
2	4.11835D-03	4.97364D+00	1.85700D-01	7.70725D-01	4.32493D-01	2.65790D-02	"
3	5.32323D-02	2.46267D+00	9.55458D-01	3.79255D-01	8.78915D-01	3.46504D-01	"
4	3.09634D-01	7.16793D-01	5.08354D+00	9.47947D-02	3.51637D+00	2.50657D+00	"
5	3.87471D-01	5.40029D-01	8.03633D+00	6.01548D-02	5.54126D+00	4.11340D+00	"
1	5.89456D-04	7.74088D+00	5.63002D-02	1.19981D+00	2.77822D-01	3.80305D-03	$h=\tau/4=7.75000D-02$
2	4.11835D-03	4.97364D+00	1.85700D-01	7.70714D-01	4.32499D-01	2.65783D-02	"
3	5.32323D-02	2.46267D+00	9.55458D-01	3.79121D-01	8.79227D-01	3.46258D-01	"
4	3.09634D-01	7.16793D-01	5.08354D+00	9.386900-02	3.55105D+00	2.45734D+00	"
5	3.87471D-01	5.40029D-01	8.03633D+00	5.87489D-02	5.67387D+00	3.91840D+00	"

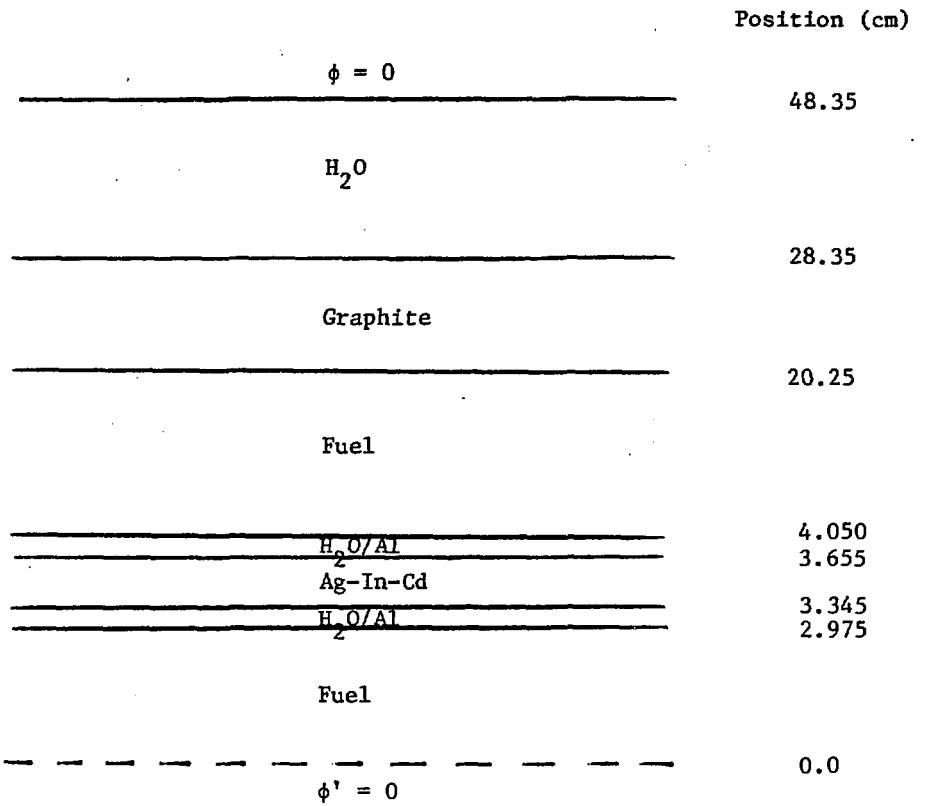

Fig. 4. Asymmetric Ag-In-Cd Slab Model

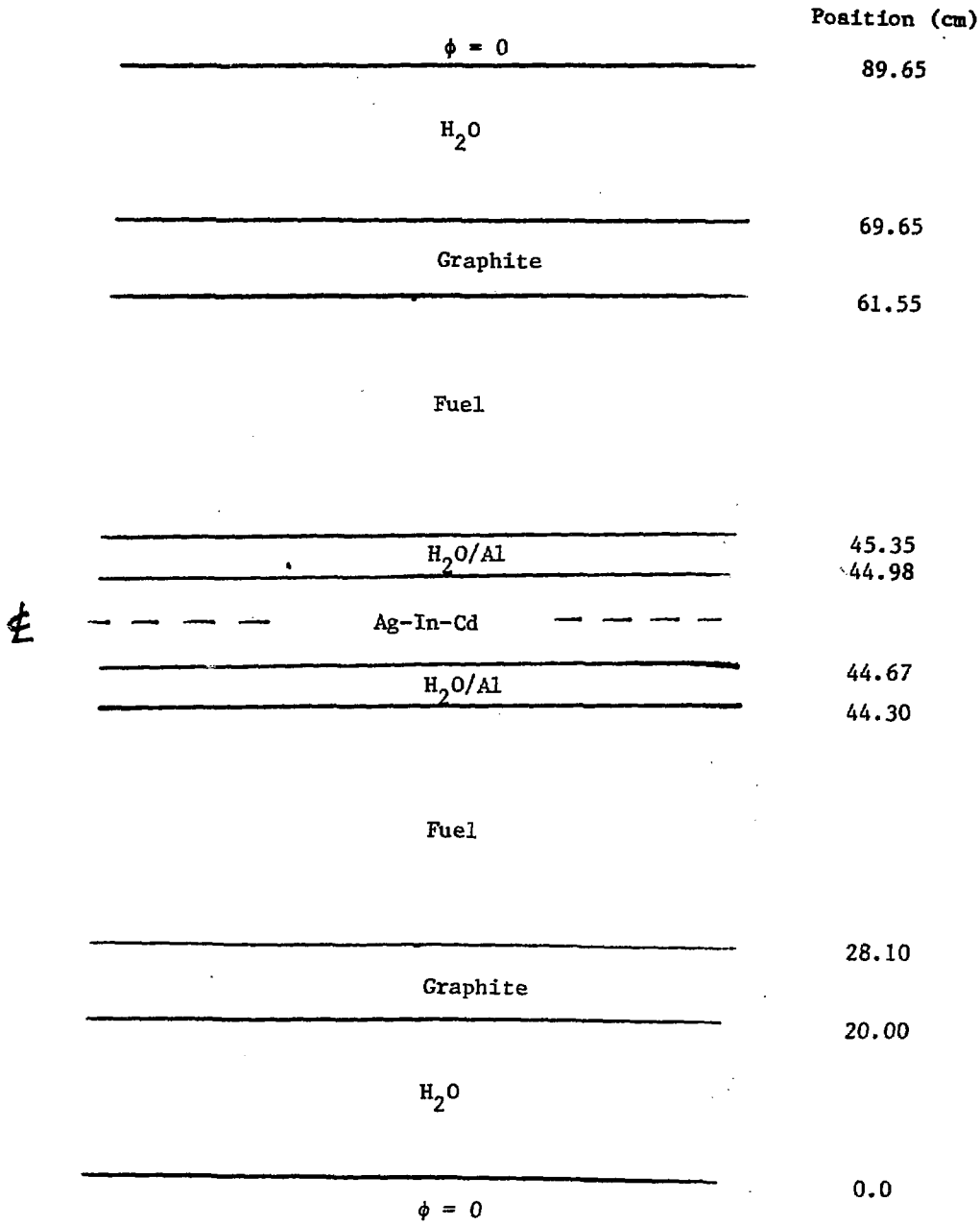

Fig. 5. Symmetric Ag-In-Cd Slab Model

Table IX. Eigenvalue Calculations for One-Dimensional Reactor Slab Models with Ag-In-Cd Blades.

Model	Ag-In-Cd Blade Position	Code	h cm	k_{eff}	Comments
Fig. 4 (Asymm.)	Out	ONEDANT		1.5379	P_1, S_8 Calc.
Fig. 4	Out	DIF3D		1.5352	
Fig. 4	In	ONEDANT		1.3200	P_1, S_8 Calc.
Fig. 4	In	DIF3D	$h=\tau$	1.3208	Σ_a, D from $\langle\alpha(P_5)\rangle$ and $\langle\beta(P_5)\rangle$
"	"	"	$h=\tau/2$	1.3208	"
"	"	"	$h=\tau/3$	1.3208	"
"	"	"	$h=\tau/4$	1.3208	"
Fig. 4	In	DIF3D		1.3688	$\langle\alpha(P_5)\rangle$ Internal B.C.'s
Fig. 5 (Symm.)	Out	ONEDANT		1.5093	P_1, S_8 Calc.
Fig. 5	Out	DIF3D		1.5050	
Fig. 5	In	ONEDANT		1.3689	P_1, S_8 Calc.
Fig. 5	In	DIF3D	$h=\tau$	1.3688	Σ_a, D from $\langle\alpha(P_5)\rangle$ and $\langle\beta(P_5)\rangle$
"	"	"	$h=\tau/2$	1.3688	"
"	"	"	$h=\tau/3$	1.3688	"
"	"	"	$h=\tau/4$	1.3688	"
Fig. 5	In	DIF3D		1.3691	$\langle\alpha(P_5)\rangle$ Internal B.C.'s

Table X. Consistency Check of Ag-In-Cd Blackness Coefficients (Asymmetric Slab Model with $h=\tau/2$).

Quantity	Group 3	Group 4	Group 5
ϕ_ℓ	17.1776	1.4671	3.8416
J_ℓ	0.61820	0.44085	1.4615
ϕ_r	17.4218	1.5321	4.1866
J_r	1.2199	0.48740	1.6478
$(J_\ell+J_r)/(\phi_\ell+\phi_r)$	0.05313	0.3095	0.3873
$\langle\alpha(P_5)\rangle$	0.05323	0.3096	0.3875
Ratio	0.9981	0.9997	0.9995
$(J_\ell-J_r)/(\phi_\ell-\phi_r)$	2.4637	0.7167	0.5400
$\langle\beta(P_5)\rangle$	2.4627	0.7168	0.5400
Ratio	1.0004	0.9999	1.0000

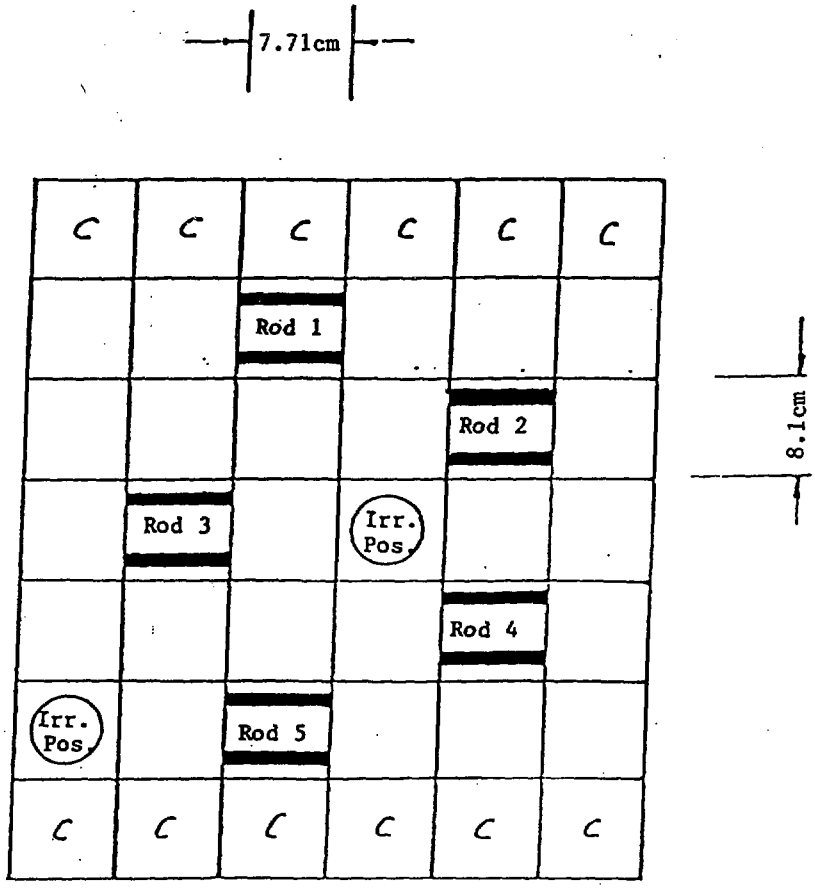

Fig. 6. Locations of the Ag-In-Cd Control Blades in the 10-MW Generic Reactor.

Table XI. XYZ Calculations for the 10-MW Generic Reactor for Fresh LEU U_3Si_2 Fuel with Ag-In-Cd Control Blades.

Rod Configuration	Code	h cm	k_{eff}	$\Delta\rho$** %
All Out	VIM		1.1922±0.0031	
All Out	DIF3D		1.1903	
All In	VIM		1.0296±0.0031	13.25±0.36
All In	DIF3D*	$h=\tau/2$	1.0309	12.99
Rod 3 Out	VIM		1.0838±0.0033	8.39±0.36
Rod 3 Out	DIF3D*	$h=\tau$	1.0790	8.66
Rod 3 Out	DIF3D*	$h=\tau/2$	1.0813	8.47
Rod 3 Out	DIF3D*	$h=\tau/3$	1.0818	8.43
Rod 3 Out	DIF3D*	$h=\tau/4$	1.0816	8.44

*Based on the Ag-In-Cd blackness-modified diffusion parameters.

**$\Delta\rho \equiv (k_{out} - k_{in})/k_{out}k_{in}$.

9.3 Hafnium Control Elements

Control elements for the Japanese 20-MW JRR-3 reactor consist of water-filled natural hafnium boxes 6.36 cm on a side and with walls 0.50 cm thick. They are illustrated in Fig. 7.

Natural hafnium is a strong resonance absorber, as Fig. 8 (from Ref. 16) shows. Since the EPRI-CELL library does not contain resonance information for the hafnium isotopes and because of the flat flux approximation used by EPRI-CELL for fast and epithermal cross sections, only the thermal fine-group cross sections were used in the evaluation of the blackness coefficients. The non-thermal cross sections were generated by the MC^2-2 Code[13] which rigorously treats resolved resonance absorption. Shown below is the assumed composition of the natural hafnium control material of density 13.3 g/cm^3.

Hafnium Composition

Isotope	Abundance, %	Atoms/barn-cm
174	0.16	7.1797E-05
176	5.20	2.3334E-03
177	18.60	8.3464E-03
178	27.10	1.2161E-02
179	13.74	6.1656E-03
180	35.20	1.5795E-02

With these fine-group macroscopic hafnium cross sections, Eqs. (1) and (2) were numerically integrated to obtain the reflection and transmission coefficients using ONEDANT[2] values for the angular fluxes on the surfaces of a 0.50-cm-thick hafnium slab. From these reflection and transmission coefficients, the fine-group blackness coefficients were evaluated by the methods described in Section 5. The broad-group coefficients, $\langle\alpha\rangle$ and $\langle\beta\rangle$, were obtained by weighting the fine-group values by means of the surface fluxes, as described in Section 6.

Table XII summarizes the broad-group blackness coefficients for natural hafnium calculated in the P_1, P_3, P_5, and "dirty blackness" approximations. This table also shows that $\Sigma_a/\Sigma_s \ll 1$ for groups 1 and 2 and, therefore, blackness theory is needed only for groups 3, 4, and 5. The effective diffusion parameters corresponding $\langle\alpha\ (P_5)\rangle$ and $\langle\beta\ (P_5)\rangle$ were calculated from Eqs. (30-32) for mesh interval spacings of $h = \tau$, $\tau/2$, $\tau/3$, and $\tau/4$. They are shown in Table XIII.

These effective diffusion parameters, for $h = \tau/2$, were first applied to a 1D cell calculation with reflective boundary conditions (See Fig. 9.). Using diffusion theory, eigenvalues were calculated for hafnium in the cell and for water replacing the hafnium slab. For these calculations blackness-modified hafnium diffusion parameters were used for groups 3, 4, and 5. VIM[14]/ Monte Carlo calculations were made for the same cell problem. Generally speaking, the fine-group macroscopic hafnium cross sections obtained by VIM were found to be in good agreement with those obtained by the MC^2/EPRI-CELL

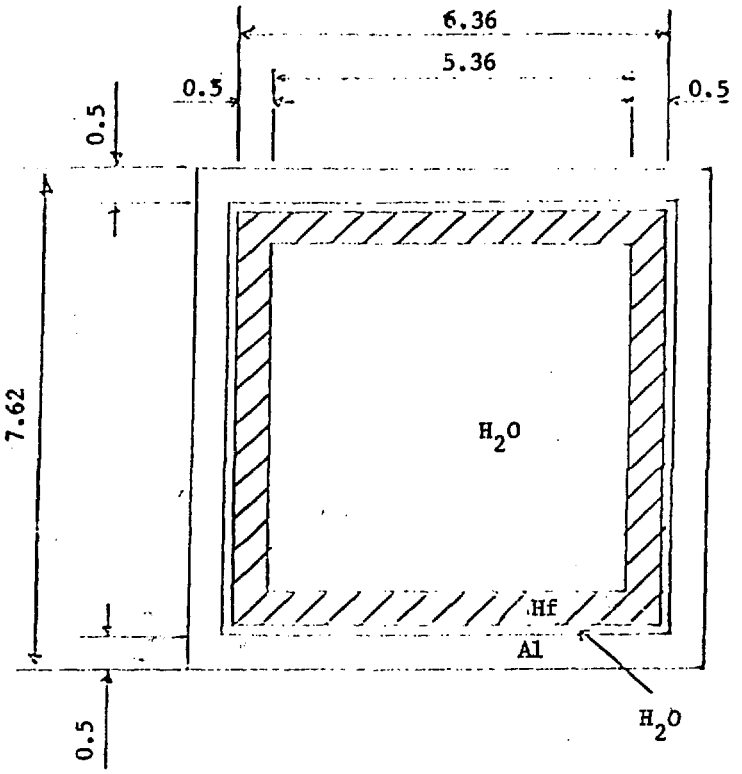

Fig. 7. Hafnium Control Element for the JRR-3 Reactor. All dimensions in cm.

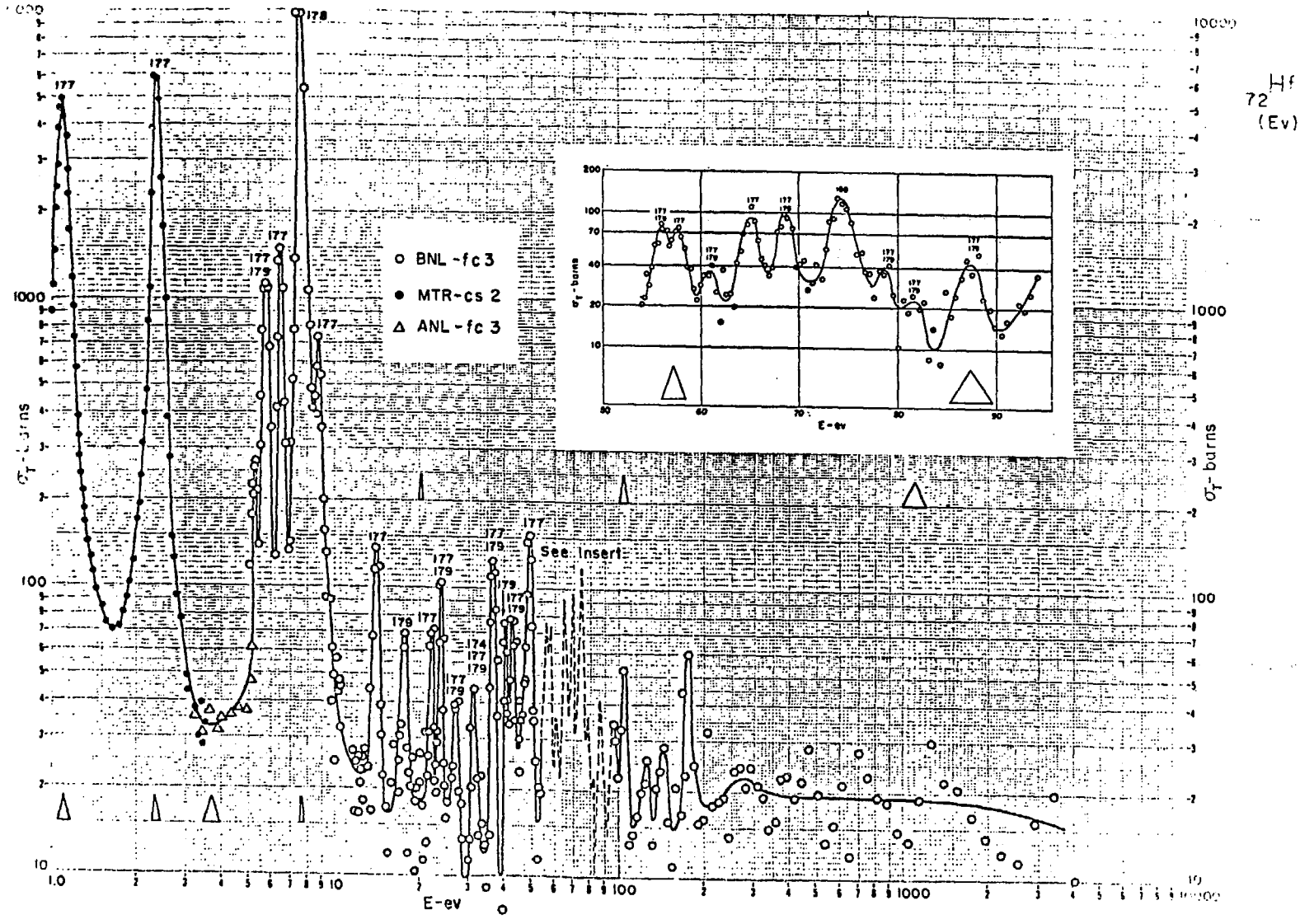

Fig. 8. Total Neutron Cross Section for Natural Hafnium (from Ref. 16).

Table XII. Broad-Group Blackness Coefficients for a 0.50-cm-Thick Natural Hafnium Slab.

Quantity	Group 1	Group 2	Group 3	Group 4	Group 5
E_u (eV)	1.0E+07	8.208E+05	5.531E+03	1.855	0.6249
Σ_a/Σ_s	0.01075	0.05192	0.6362	11.1581	6.5293
$\Sigma_a\tau$	1.6286E-03	1.1406E-02	2.3999E-01	2.6010	1.4916
No. of Fine Groups	1	1	32	14	21
$\alpha(P_1)$	8.1451E-04	5.6485E-03	1.0356E-01	4.5802E-01	3.8305E-01
$\alpha(P_3)$	8.1413E-04	5.6328E-03	1.0046E-01	4.3288E-01	3.6102E-01
$\alpha(P_5)$	8.1410E-04	5.6316E-03	1.0016E-01	4.3074E-01	3.5886E-01
$\langle\alpha(P_5)\rangle$	8.1410E-04	5.6316E-03	1.0208E-01	4.1096E-01	3.5165E-01
$\langle\alpha(DB)\rangle$*	7.6051E-04	5.2312E-03	1.0070E-01	4.1707E-01	3.5647E-01
$\beta(P_1)$	4.3542	2.8878	1.1282	5.1022E-01	5.8520E-01
$\beta(P_3)$	4.3541	2.8869	1.1191	4.8566E-01	5.6261E-01
$\beta(P_5)$	4.3541	2.8868	1.1179	4.8394E-01	5.6093E-01
$\langle\beta(P_5)\rangle$	4.3541	2.8868	1.2135	5.1162E-01	5.7023E-01
$\langle\beta(DB)\rangle$*	3.8416E+02	5.4857E+01	4.8787	5.3505E-01	6.2356E-01

*Weighted average of the "dirty blackness" (DB) coefficients (see Eqs. 26 and 27).

Table XIII. Natural Hafnium P_5 Effective Diffusion Parameters for Mesh-Centered Fluxes with Fine-Group-Weighted α and β.

Group	$\langle\alpha\rangle$	$\langle\beta\rangle$	k	D_{eff}	Σ_{tr}	$\Sigma_{a_{eff}}$	h(cm)
1	8.14101D-04	4.35410D+00	5.46987D-02	1.08853D+00	3.06225D-01	3.25701D-03	$h=\tau=5.00000D-01$
2	5.63162D-03	2.88677D+00	1.76788D-01	7.21693D-01	4.61877D-01	2.25705D-02	"
3	1.02082D-01	1.21349D+00	1.19444D+00	3.03372D-01	1.09876D+00	4.45834D-01	"
4	4.10961D-01	5.11615D-01	5.81127D+00	1.27904D-01	2.60612D+00	8.35548D+00	"
5	3.51649D-01	5.70234D-01	4.23606D+00	1.42559D-01	2.33822D+00	3.66947D+00	"
1	8.14101D-04	4.35410D+00	5.46987D-02	1.08847D+00	3.06239D-01	3.25671D-03	$h=\tau/2=2.50000D-01$
2	5.63162D-03	2.88677D+00	1.76788D-01	7.21340D-01	4.62103D-01	2.25485D-02	"
3	1.02082D-01	1.21349D+00	1.19444D+00	2.96852D-01	1.12290D+00	4.26669D-01	"
4	4.10961D-01	5.11615D-01	5.81127D+00	9.23179D-02	3.61071D+00	3.70609D+00	"
5	3.51649D-01	5.70234D-01	4.23606D+00	1.15411D-01	2.88824D+00	2.27189D+00	"
1	8.14101D-04	4.35410D+00	5.46987D-02	1.08846D+00	3.06242D-01	3.25665D-03	$h=\tau/3=1.66667D-01$
2	5.63162D-03	2.88677D+00	1.76788D-01	7.21275D-01	4.62144D-01	2.25444D-02	"
3	1.02082D-01	1.21349D+00	1.19444D+00	2.95636D-01	1.12751D+00	4.23176D-01	"
4	4.10961D-01	5.11615D-01	5.81127D+00	8.49782D-02	3.92257D+00	3.10126D+00	"
5	3.51649D-01	5.70234D-01	4.23606D+00	1.10066D-01	3.02850D+00	2.05846D+00	"
1	8.14101D-04	4.35410D+00	5.46987D-02	1.08846D+00	3.06243D-01	3.25663D-03	$h=\tau/4=1.25000D-01$
2	5.63162D-03	2.88677D+00	1.76788D-01	7.21252D-01	4.62159D-01	2.25430D-02	"
3	1.02082D-01	1.21349D+00	1.19444D+00	2.95212D-01	1.12913D+00	4.21958D-01	"
4	4.10961D-01	5.11615D-01	5.81127D+00	8.23438D-02	4.04807D+00	2.90527D+00	"
5	3.51649D-01	5.70234D-01	4.23606D+00	1.08169D-01	3.08159D+00	1.98679D+00	"

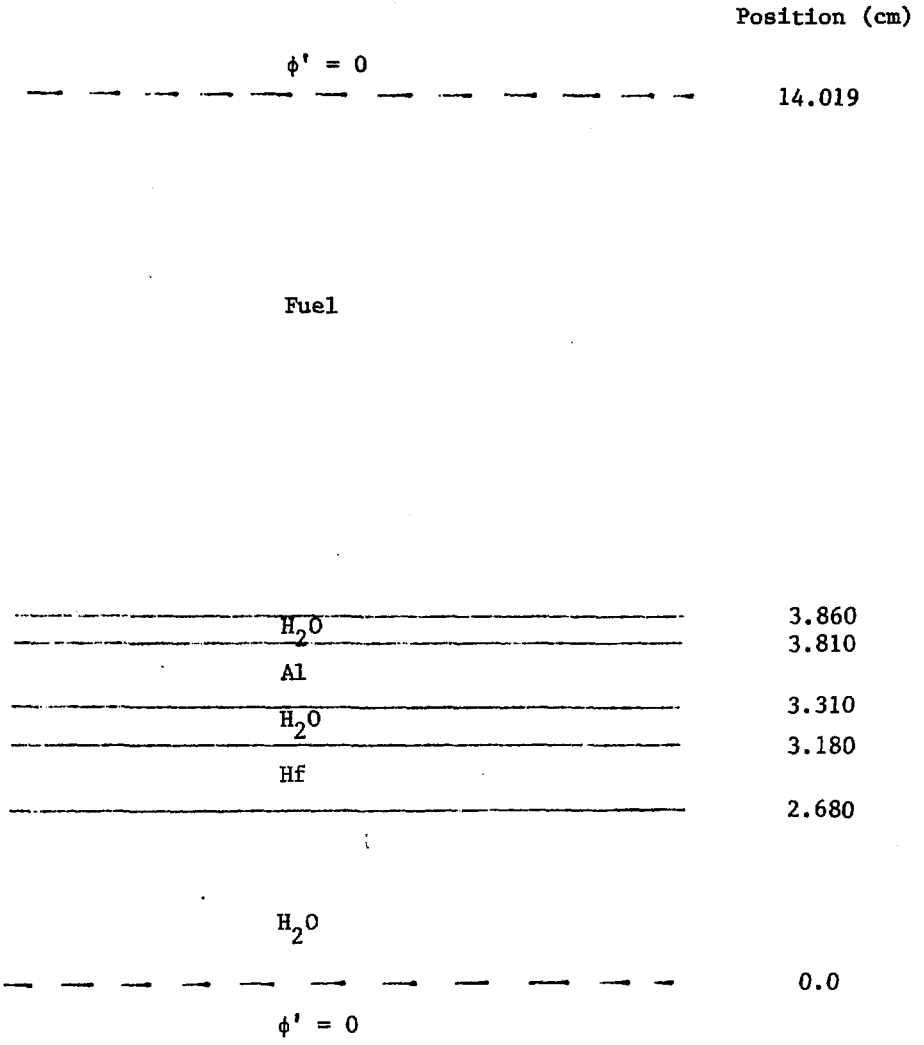

Fig. 9. One-Dimensional Hafnium Cell With Reflective Boundary Conditions.

combination. Eigenvalues from the two sets of calculations are compared in Table XIV. For reasons which do not appear to be related to the values of the hafnium blackness coefficients, the DIF3D eigenvalues for both the rod-in and the rod-out configurations are higher than those from the corresponding VIM calculations by about 1.4%. The worth of the hafnium rod based on blackness-modified diffusion theory is within 1.6 standard deviations of the VIM result. Had the blackness coefficients been based on the VIM broad-group cross sections, the worth values would have agreed within one standard deviation.

The effective diffusion parameters shown in Table XIII for $h = \tau/2$ were used to calculate the worth of the hafnium control rods in the JRR-3 reactor in an XYZ calculation. Figure 10 shows a sketch of the JRR-3 reactor,[17] and the geometry of the hafnium control element is given in Fig. 7. The standard fuel element consists of 20 plates with 16 plates in the control rod follower element. For the purpose of these calculations, the fuel was assumed to consist of fresh LEU. In addition to the 3D blackness-modified diffusion calculations, detailed Monte Carlo analyses were performed. DIF3D and VIM eigenvalues and rod worths are compared in Table XV. As with the 1D cell problem, blackness-modified hafnium diffusion parameters were used only for groups 3, 4, and 5. For the rods half-way withdrawn, the DIF3D eigenvalue is 0.73% larger than the VIM result whereas for the rods fully-inserted the DIF3D value is 0.84% smaller than the VIM calculation. Since the same effective diffusion parameters were used for both of the DIF3D calculations, it appears that this cross-over in k_{eff} relative to VIM is not due to the blackness coefficients.

Table XIV. Eigenvalues and Hafnium Worths for One-Dimensional Cell Calculations.

Code	Rod-In k_{eff}	Rod-Out k_{eff}	$\Delta\rho$* %
VIM	1.0305±0.0024	1.3388±0.0031	22.34±0.29
DIF3D	1.0460	1.3562	21.87

*$\Delta\rho \equiv (k_{out} - k_{in})/k_{out}\, k_{in}$.

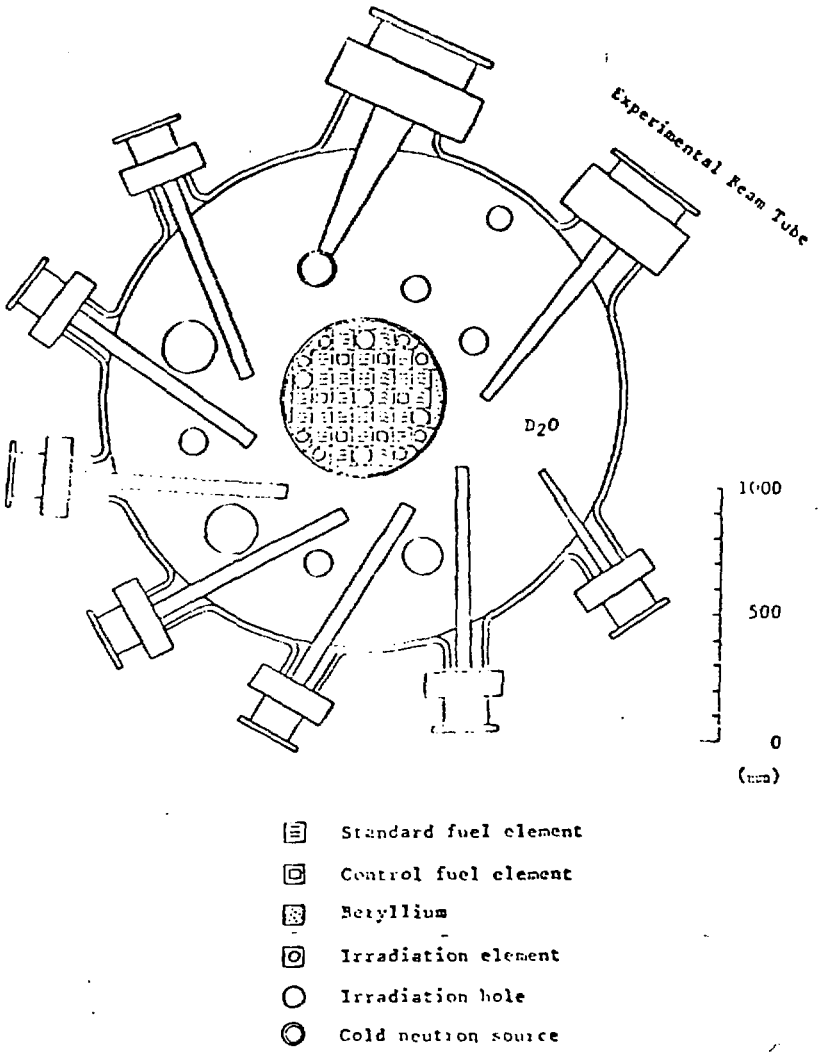

Fig. 10. Horizontal Cross Section of JRR-3(M).

Table XV. Eigenvalues and Hafnium Control Rod Worths in the JRR-3 Reactor.

Rod Config.	k_{eff} DIF3D	$\Delta\rho^*$ %	k_{eff} VIM	$\Delta\rho^*$ %
All out	1.2291		1.2227±0.0023	
At 50%	1.1224	7.74	1.1143±0.0024	7.96±0.25
All In	0.8689	33.74	0.8763±0.0028	32.33±0.39

*$\Delta\rho \equiv (k_{out} - k)/k_{out}\ k$.

10. TWO-AND-THREE DIMENSIONAL CONTROL RODS

The primary purpose of this report was to present a set of procedures for calculating control rod worths for a special class of control elements — those that can be approximated by a one-dimensional slab treatment. For this class of problems, a pair of blackness coefficients was evaluated which depends only on the characteristics of the control material and from which effective diffusion parameters are determined. In the more general case of two or more dimensions, however, quantities analogous to α and β do not exist. For this general case the assumption is made that effective diffusion parameters for the strong absorber can be found which depend primarily on the cross sections of the absorber, its dimensions, and the mesh spacing used in diffusion theory to describe the region but do not depend on the environment outside the lumped absorber.

Unmodified diffusion parameters may be used for those groups for which $\Sigma_a \ll \Sigma_s$. The following procedure may be used to determine the effective diffusion parameters for the other groups of the lumped absorber.

1. An arbitrary relationship between D_{eff} and $\Sigma_{a_{eff}}$ is defined. For example, Hannum[11] suggests using

$$D_{eff} = \frac{1}{3\,\Sigma_{a_{eff}}} .$$

2. A characteristic model cell with reflecting boundary conditions is defined. This cell contains the lumped absorber, its immediate environment, and a homogenized fuel zone.

3. For this cell a fine mesh high-order transport or Monte Carlo calculation is performed to determine for each energy group the capture rate in the homogenized control region relative to the fission rate in the fuel region. It may be necessary to divide the absorber into several nested regions and to generate appropriate cross sections for each region for the transport calculations.

4. The same cell is used for a diffusion-theory calculation choosing the same mesh structure which will be used later for global diffusion calculations.

5. The diffusion-theory calculations are repeated using different sets of Σ_a and D values for the homogenized control region. For each case and for each energy group the capture rate in the absorber is determined relative to the fission rate in the fuel. Effective diffusion parameters are those values of Σ_a and D for the control region which produce the same reaction rate ratios as those obtained from the transport or Monte Carlo calculations.

6. Control rod worths are determined by performing global diffusion calculations with and without the control rod inserted using the above group-dependent values for $\Sigma_{a_{eff}}$ and D_{eff}.

This procedure for determining $\Sigma_{a_{eff}}$ and D_{eff} by matching reaction rate ratios was used to calculate the worths of the borated-steel shim-safety rods in the University of Michigan Ford Nuclear Reactor (FNR).[18] The geometry and composition of the shim-safety rods are shown in Fig. 11. It is obvious from this figure that the FNR shim-safety rods do not lend themselves to a one-dimensional slab treatment.

Fig. 11. FNR Shim-Safety Rod Geometry and Composition

Geometry

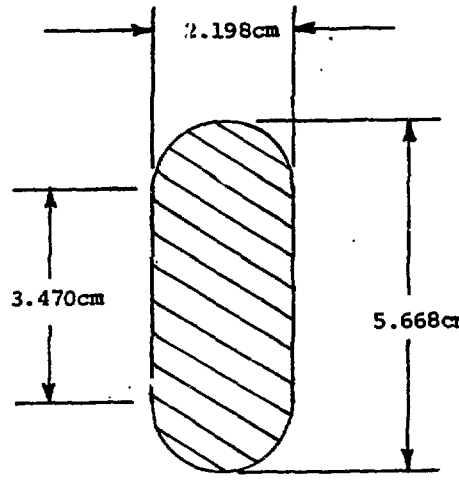

Composition

(Boron stainless steel, 1.5 w/o natural boron)

Isotope/Element	Atoms/barn-cm
^{10}B	0.001108
^{11}B	0.005184
Cr	0.0164
Fe	0.05644
Ni	0.0113

Figure 12 shows an XY model of the FNR 27-element fresh LEU core configuration in which shim-safety rod worth measurements were made. Diagrams of the standard and control LEU UAl_x fuel elements are given in Fig. 13.

VIM-Monte Carlo calculations were performed for a control cell consisting of the borated-steel rod and the control fuel element surrounded on each side by one half of a standard fuel assembly. For these calculations reflective boundary conditions were used and each fuel slab, side plate, clad plate, water channel, and the control rod were explicitly represented. Results were collapsed into the standard five-group structure shown at the top of Table III. Group-wise reaction rates were edited over the control region, the two core regions, and the side-plate regions shown in Fig. 14. For each group the reaction rate ratio of absorption in the control rgion to fission in the core regions was determined.

Cross sections for each homogenized region shown in Fig. 14 were generated by EPRI-CELL. The mesh structure used in the XY diffusion calculations of the control cell (Fig. 14) was the same as that used later in the full core model (Fig. 12). Beginning with the highest energy groups, Σ_a and D in the control region were adjusted until the diffusion-theory calculation for the reaction rate ratio, R_a (Control Region)/R_f (cell), matched that determined by the VIM-Monte Carlo calculations for each energy group. For the purpose of modifying D, it was assumed that only Σ_a changed in the expression for the macroscopic transport cross section, $\Sigma_{tr} = \Sigma_a - \Sigma_s(1 - \mu)$.

Having thus determined the group-dependent effective diffusion parameters for the homogenized control region, FNR control rod worths were evaluated using the DIF3D code and the XY odel shown in Fig. 12. For these calculations it was assumed that the non-borated-steel regulating rod in grid postion 28 was fully withdrawn. The results are summaried in Table XVI and are compared with the measured values of the worths of the shim-safety rods. It is seen that the measured and calculated worths are in very satisfactory agreement.

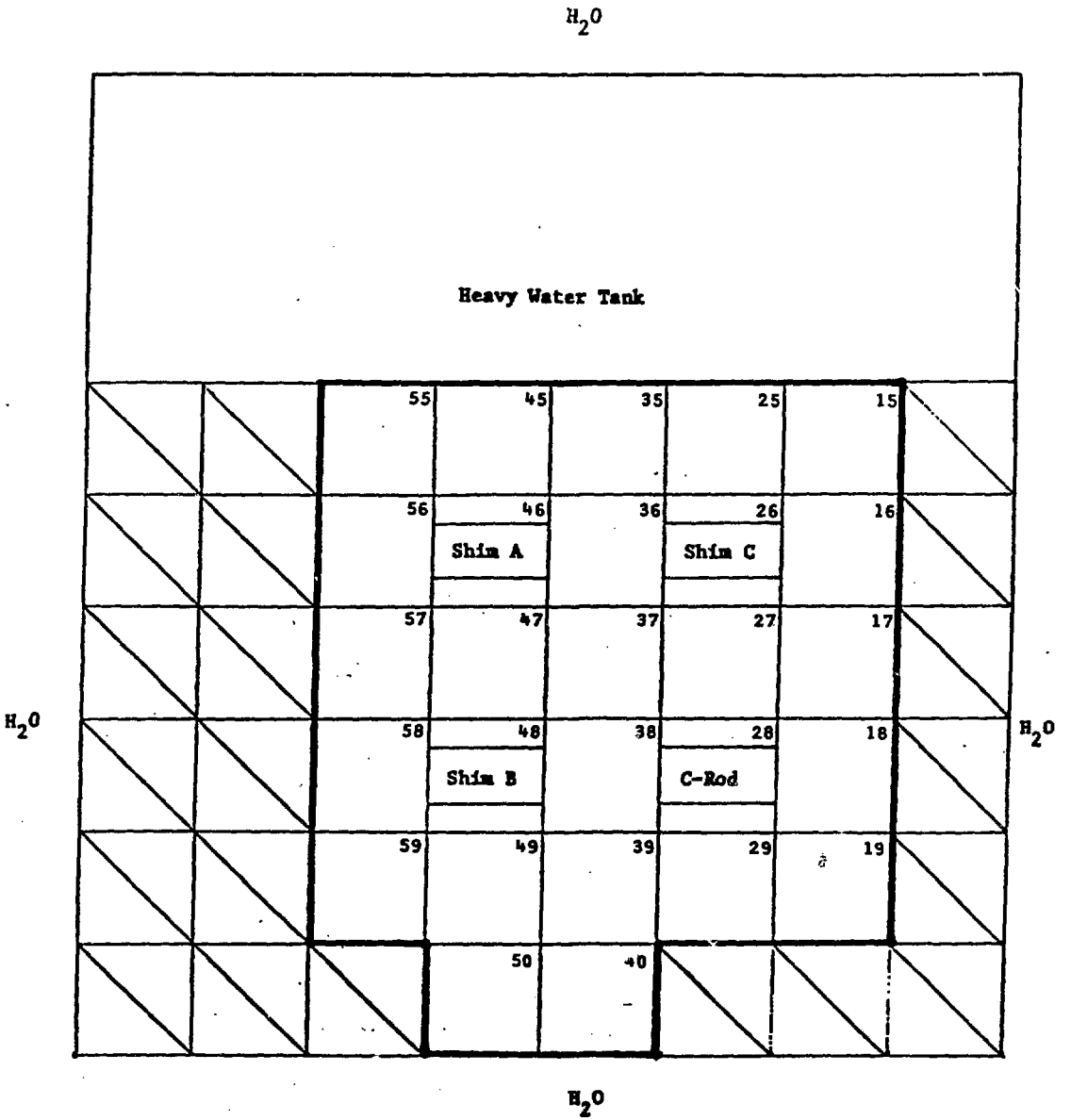

Fig. 12. FNR 27-Element LEU Core for Shim-Safety Rod Worth Measurements

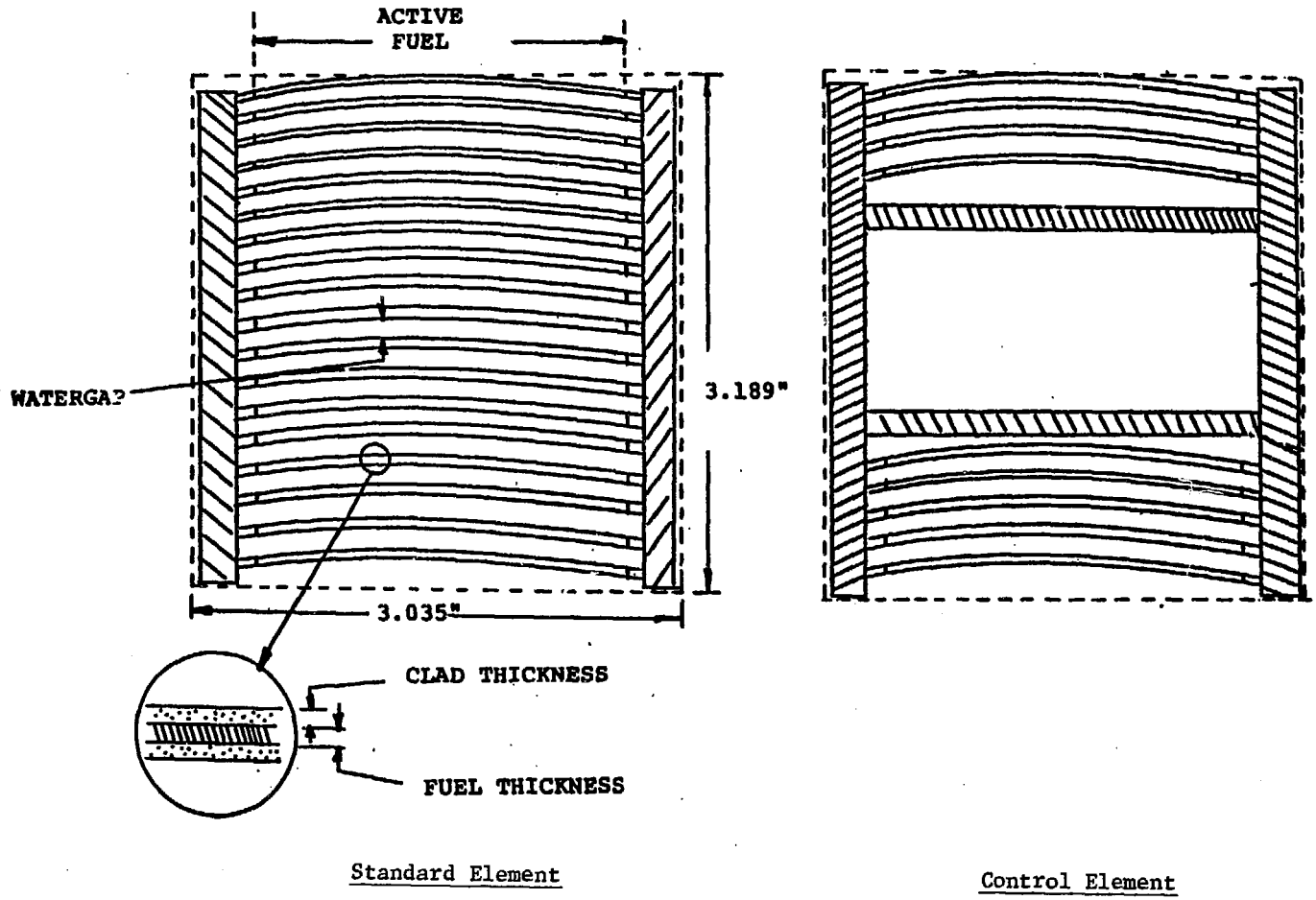

Fig. 13. FNR Standard and Control Fuel Elements

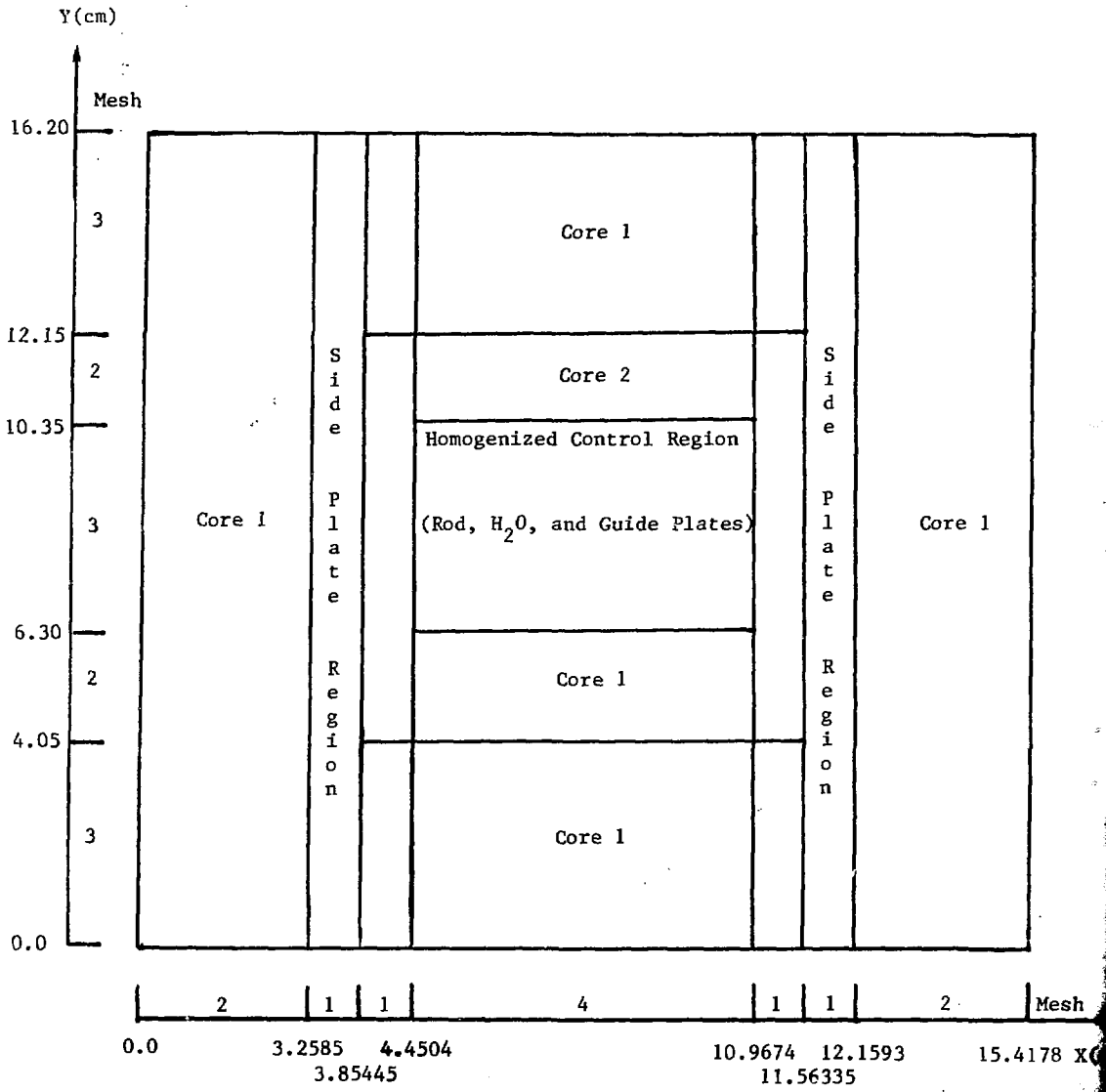

Fig. 14. XY Cell with Reflecting Boundaries for Calculating Effective Diffusion Parameters in Control Region.

Table XVI. FNR Shim-Safety Rod Worths for 27 Fresh LEU Fuel Element Core

Rod Configuration	Grid Position	k_{eff}	Reactivity Worth, % Δk/k Measured E	Calculated C	C/E Ratio
All Out		1.02208			
A In	46	0.99910	2.22	2.25	1.01
B In	48	0.99782	2.32	2.38	1.02
C In	26	0.99944	2.28	2.22	0.97

11. CONCLUSIONS

There are several important underlying assumptions upon which blackness theory rests. These are:

1. The control slab can be adequately described by the monoenergetic, one-dimensional, Boltzmann transport equation.

2. There can be no sources (fission, scattering, or n,2n) in the control material.

3. The thickness of the absorber slab is very small relative to the transverse dimensions.

4. Scattering within the slab is isotropic.

5. Diffusion theory is applicable to regions outside the control slab.

If these conditions are met reasonably well and if good, self-shielded, cross section data are available for the control slab, the fine-group-weighted blackness coefficients, $\langle\alpha(P_5)\rangle$ and $\langle\beta(P_5)\rangle$, can be expected to yield accurate eigenvalues when used in a diffusion-theory calculation. For this purpose effective diffusion parameters for the control slab can be determined in terms of the blackness coefficients and the mesh interval width.

Those fast energy groups for which $\Sigma_s >> \Sigma_a$ in the control slab may be treated with normal diffusion theory. "Dirty blackness theory" provides a good approximation for $\langle\alpha\rangle$ and $\langle\beta\rangle$ for those thermal groups for which $\Sigma_a >> \Sigma_s$. However, β is very sensitive to the effects of neutron scattering and so the "dirty blackness" approximation should not be applied to the epithermal groups.

If the geometry of the control rods does not lend itself to a thin slab approximation, α and β blackness coefficients do not exist. Other methods must then be used to determine effective diffusion parameters for the control material. One such method is to define a representative control cell and to determine by a Monte Carlo or high-order transport calculation the capture rate in the absorber relative to that in a nearby fuel region for each energy group. For the same cell D and Σ_a of the control material are adjusted so that a diffusion-theory calculation gives the same values for the reaction rate ratios. Results in good agreement with the measured values were obtained by this method for the FNR shim-safety rods.

ACKNLOWLEDGEMENTS

There are many persons who have made important contributions to this study. E. M. Gelbard showed how mesh-dependent effective diffusion parameters can be expressed in terms of the blackness coefficients. R. B. Pond did the diffusion calculations for the R2 and JRR-3 reactors and K. E. Freese provided similar information for the IAEA 10-MW Generic Reactor. Nearly all the Monte Carlo calculations were done by R. M. Lell. The contributions from each of these individuals is most gratefully acknowledged.

References

1. C. W. Maynard, "Blackness Theory and Coefficients for Slab Geometry," Nucl. Sci. Eng. 6, 174 (1959). Also, C. W. Maynard, "Blackness Theory for Slabs," in Naval Reactors Physics Handbook, Vol. I, A. Radkowsky, Editor, pp. 409-448, U.S. AEC (1964).

2. R. D. O'Dell, F. W. Brinkley, and D. R. Marr, "User's Manual for ONEDANT: A Code Package for One-Dimensional, Diffusion-Accelerated, Neutral-Particle Transport," LA-9184-M (February 1982).

3. F. B. Hildebrand, Introduction to Numerical Analysis, McGraw-Hill Book Company, Inc., 1956, see Chap. 8.

4. C. W. Maynard, "Blackness Theory and Coefficients for Slab Geometry," WAPD-TM-168 (May 1959).

5. M. Abramowitz and I. A. Stegun, Eds., Handbook of Mathematical Functions with Formulas, Graphs, and Mathematical Tables, National Bureau of Standards Applied Mathematics Series #55, U.S. Government Printing Office (March 1965).

6. R. J. Royston, "The Behavior of a Flux of Neutrons in the Neighborhood of a Control Plate," AERE T/R 2211 (March 1957).

7. M. Goldsmith, R. T. Jones, T. M. Ryan, S. Kaplan, and A. D. Voorhis, "Theoretical Analysis of Highly Enriched Light Water Moderated Critical Assemblies," Proceedings of the Second United Nations International Conference on the Peaceful Uses of Atomic Energy, Vol. 12, pp. 435-445, United Nations, Geneva (1958).

8. K. L. Derstine, "DIF3D: A Code to Solve One, Two, and Three Dimensional Finite Difference Theory Problems," ANL-82-64, April 1984.

9. B. Davison and J. B. Sykes, Neutron Transport Theory, Oxford University Press (1957).

10. B. A. Zolotar, et al., "EPRI-CELL Description," Advanced Recycle Methodology Program System Documentation, Part II, Chapter 5, Electric Power Research Institute (September 1977). EPRI-CELL code supplied to Argonne National Laboratory by Electric Power Research Institute, Palo Alto, California (1977).

11. W. H. Hannum, "Representation of Plate Self-Shielding in Diffusion Theory," in Naval Reactors Physics Handbook, Vol. I, A. Radkowsky, Editor, pp. 595-620, U.S. AEC (1964).

12. A. F. Henry, "A Theoretical Method for Determining The Worth of Control Rods," Bettis Atomic Power Division Report WAPD-218 (August 1959).

13. H. Henryson II, B. J. Toppel, and C. G. Stenberg, "MC^2-2: A Code to Calculate Fast Neutron Spectra and Multigroup Cross Sections," ANL-8144, June 1976.

14. R. E. Prael and J. J. Milton, "A User's Manual for the Monte Carlo Code VIM," FRA-TM-84 (February 20, 1976).

15. "Research Reactor Core Conversion from the Use of Highly Enriched Uranium to the Use of Low Enriched Uranium Fuels Guidebook," IAEA-TECDOC-233, Vienna (1980).

J. E. Matos, K. E. Freese, and W. L. Woodruff, Comparison of Safety Parameters and Transient Behavior of a 10-MW Reactor with HEU and LEU Fuels," Proceedings of the International Meeting on Reduced Enrichment for Research and Test Reactors, 24-27 October, 1983, Tokai, Japan, JAERI-M 84-073 (May 1984).

16. D. J. Hughes and R. B. Schwartz, Neutron Cross Sections, 2nd Edition, BNL 325 (July 1, 1958).

17. H. Icikawa, H. Ikawa, H. Ando, M. Takayagi, H. Tsuruta, and Y. Miyasaka, "Neutronic and Thermo-Hydraulic Design of JRR-3(M) Reactor," Proceedings of the International Meeting on Reduced Enrichment for Research and Test Reactors," 24-27 October, 1983, Tokai, Japan (May 1984).

18. W. Kerr, "Low Enrichment Fuel Evaluation and Analysis Program," Summary Report for the Period January 1979 - December 1979. University of Michigan, Department of Nuclear Engineering (January 1980).

Distribution for ANL/RERTR/TM-5

Internal:

A. Schriesheim
C. E. Till
R. Avery
L. Burris
D. W. Cissel
P. I. Amundson
F. Y. Fradin
J. H. Kittel
L. G. LeSage
R. A. Lewis
R. J. Teunis
D. C. Wade
S. K. Bhattacharyya
E. M. Gelbard
A. Travelli (100)
R. F. Domagala
G. L. Hofman
L. A. Neimark
J. Rest
D. R. Schmitt
C. Steves
H. R. Thresh
T. Wiencek
J. A. Zic
ANL Contract File
ANL Patent Dept.
ANL Libraries (3)
TIS Files (6)

External:

DOE-TIC, for distribution per UC-83 (83)
Manager, Chicago Operations Office, DOE
Director, Technology Management Div., DOE-CH
Applied Physics Division Review Committee:
- E. L. Draper, Jr., Gulf States Utilities, Beaumont, Tex.
- J. F. Jackson, Los Alamos National Lab.
- W. E. Kastenberg, U. California, Los Angeles
- D. A. Meneley, U. New Brunswick, Fredericton
- J. E. Meyer, Massachusetts Inst. Technology
- N. J. McCormick, U. Washington
- A. E. Wilson, Idaho State U.

Materials Science and Technology Division Review Committee:
- C. B. Alcock, U. Toronto
- A. Arrott, Simon Fraser U.
- R. C. Dynes, Bell Lab., Murray Hill
- A. G. Evans, U. California, Berkeley
- H. K. Forsen, Bechtel Group, Inc., San Francisco
- E. Kay, IBM San Jose Research Lab.
- M. B. Maple, U. California, San Diego
- P. G. Shewmon, Ohio State U.
- J. K. Tien, Columbia U.
- J. W. Wilkins, Cornell U.